



NIH Public Access

Author Manuscript

Biomacromolecules. Author manuscript; available in PMC 2012 April 28.

Published in final edited form as:

Biomacromolecules. 2008 November ; 9(11): 3294–3307. doi:10.1021/bm800876v.

Effects of the Incorporation of a Hydrophobic Middle Block into a PEG-Polycation Diblock Copolymer on the Physicochemical and Cell Interaction Properties of the Polymer-DNA Complexes

Rahul Sharma[†], Jae-Sung Lee[†], Ryan C. Bettencourt[‡], Chuan Xiao[‡], Stephen F. Konieczny[‡], and You-Yeon Won^{†,*}

[†]School of Chemical Engineering, Purdue University, West Lafayette, Indiana 47907

[‡]Department of Biological Sciences, Purdue University, West Lafayette, Indiana 47907

Abstract

One-component homopolymers of cationic monomers (polycations) and diblock copolymers comprising poly(ethylene glycol) (PEG) and a polycation block have been the most widely used types of polymers for formulation of polymer-based gene delivery systems. In this study, we incorporate a hydrophobic middle block into the conventional PEG-polycation architecture, and investigate the effects of this hydrophobic modification on the physicochemical and cell-level biological properties of the polymer-DNA complexes that are relevant to gene delivery applications. The ABC-type triblock copolymer used in this study consists of (A) PEG, (B) hydrophobic poly(n-butyl acrylate) (PnBA) and (C) cationic poly(2-(dimethylamino)ethyl methacrylate) (PDMAEMA) component polymers. The properties of the triblock copolymer/DNA complexes are compared with those of two other, more conventional DNA carriers derived, respectively, using a PDMAEMA homopolymer and a PEG-PDMAEMA diblock copolymer having comparable molecular weights for individual blocks. The PEG-PnBA-PDMAEMA polymer forms, in aqueous solution, positively-charged spherical micelles. The electrostatic complexation of these micelles with plasmid DNA molecules results in the formation of stable small-size DNA particles coated with a micelle monolayer, as confirmed by agarose gel electrophoresis, dynamic light scattering (DLS) and cryogenic transmission electron microscopy (cryo-TEM). Proton nuclear magnetic resonance (¹H NMR) spectroscopy measurements indicate that the whole micelle-DNA assembly (named for convenience as “micelleplex”) is shielded predominantly by the PEG chains. DLS and optical microscopy imaging measurements indicate that in comparison with PDMAEMA/DNA polyplexes, the micelleplexes have a significantly lower tendency to aggregate under physiological salt concentrations, and show reduced interactions with negatively-charged components in serum such as albumin and erythrocytes. While the micelleplexes are comparable with the PEG-PDMAEMA-based DNA polyplexes in terms of their stability against aggregation under high salt concentrations and in the presence of the albumin protein, they have a slightly higher tendency to interact with erythrocytes than the diblock copolymer polyplexes. Agarose gel electrophoresis measurements indicate that relative to the PEG-PDMAEMA polyplexes, the micelleplexes provide better protection of the encapsulated DNA from enzymatic degradation, and also exhibit greater stability against disintegration induced by polyanionic additives; in these respects, the PDMAEMA homopolymer-based polyplexes show the best performance. *In vitro* studies in HeLa cells indicate that the PDMAEMA polyplexes show the highest gene transfection efficiency among the three different gene delivery systems. Between the micelleplexes and PEG-PDMAEMA polyplexes, a higher gene transfection efficiency is

*To whom correspondence should be addressed. yywon@ecn.purdue.edu.

Supporting Information Available: This material is available free of charge via the Internet at <http://pubs.acs.org>.

observed with the latter system. All three formulations show comparable levels of cytotoxicity in HeLa cells.

1. Introduction

Gene therapy refers to the treatment of human diseases by transfer of therapeutic genes to specific cells of a patient.^{1–3} It has the potential of curing both inherited and acquired genetic disorders by supplying functional copies of the defective genes to the diseased cells. A persistent challenge in transforming this idea of gene therapy into practical medicine is the safe and effective delivery of therapeutic genes *in vivo* to targeted cells in the patient. Initially, the vast majority of gene delivery was attempted using viruses as gene carriers because of their high gene transfer efficiency. More recently, with the recognition of safety problems associated with viral vectors,⁴ the focus has shifted towards the development of non-viral delivery systems. An ideal non-viral gene carrier would be one that is capable of performing multiple functions required for the precise delivery of systemically administered DNA to the nucleus of the targeted cell; these required functions include protection of the therapeutic genes in the extracellular environment, specific cell targeting, early endosomal escape, nuclear entry, DNA release, and integration with host cell genome.^{5–8} Polymers, particularly polycations, have become very popular components of non-viral carriers for DNA because of their safety and the relative ease with which their chemical and physical properties can be tailored to meet these functional requirements for specific applications: see References 9–12 for recent reviews on this topic.

The simplest form of polymeric gene carrier can be constructed using simple polycations (i.e., polycationic homopolymers). When mixed with DNA, polycations spontaneously form complexes with DNA (“polyplexes”) due to the electrostatic interactions between the positive charges of the polycation and the negatively charged phosphate groups of DNA. While these simple polyplex-based formulations have proven to be very effective in *in vitro* gene transfer,^{13–19} they are unsuitable for *in vivo* applications because they are typically rapidly cleared from the circulation.^{3, 11} This problem of low circulation time originates from the tendency of the polyplex carriers to agglomerate or adsorb to impertinent surroundings; the high ionic strength of the serum renders them less electrostatically stable and more prone to hydrophobic aggregation, and also their positive surface charge makes them susceptible to agglomeration with negatively charged serum proteins (such as albumin and erythrocytes) and also to scavenging by macrophages which have negatively charged polyanion receptors (via phagocytosis).^{3, 20} In theory, it is possible to enhance the circulation time by coating the delivery system with biointerferent water-compatible polymers such as poly(ethylene glycol) (PEG) which can give rise to the steric stabilization of the delivery vehicle against undesirable aggregation and nonspecific electrostatic interactions with surroundings,^{21–23} the PEG-shielded polyplex structures are typically constructed by complexation of DNA with PEG-modified (“PEGylated”) polycations (i.e., polycations block or graft-copolymerized with PEG). However, these PEGylated polyplexes have been reported to prematurely dissociate under physiological environment, leading to degradation of the DNA by serum nucleases.^{24–26} This shortcoming is believed to be due largely to the strong hydrophilicity of the PEG segments²⁷ (i.e., the strong excluded-volume interaction that the PEG chains have with one another and also with the DNA molecules) which causes a significant weakening of the binding of the polycation to DNA. Also, it is known in the literature that the PEGylation of polyplexes has an inhibitive effect on the cellular uptake of the polyplexes.²⁸

Recently, there have been many reports that demonstrate the concept of multicomponent polymer-based formulations of gene delivery complexes. These polymers incorporate one or

more additional components into the PEGylated polycation platform to enhance the performances of the PEGylated polyplexes in various aspects including cellular uptake,^{29–31} endosomal escape of the polyplexes^{32–34} and timely release of the encapsulated DNA.^{35–37} In the present work, using a new triblock copolymer as the molecular building block, we explore an alternative design for constructing PEG-protected polymeric gene carriers, and compare the physicochemical and biological properties of this triblock copolymer-based gene delivery system with other more conventional polyplex formulations based on homopolymer polycations and PEG-polycation diblock copolymers. Specifically, we use an ABC-type triblock copolymer composed of (A) hydrophilic poly(ethylene glycol) (PEG), (B) hydrophobic poly(n-butyl acrylate) (PnBA) and (C) cationic poly(2-dimethylamino)ethyl methacrylate) (PDMAEMA) component blocks. Owing to this ABC sequence of blocks, the triblock copolymer self-assembles into spherical micelle-like aggregates decorated with mixed cationic and neutral corona chains in water, which can associate with and condense DNA into small particles. In this paper, we first report the preparation and characterization of the micellar assemblies of the PEG-PnBA-PDMAEMA triblock copolymer. We show that (1) when these micelles are mixed with DNA, the positively charged PDMAEMA chains in the corona primarily interact with the negatively charged phosphates on DNA, and a monolayer-thick micelle coating can be created at the outer surface of collapsed DNA, and (2) the resultant triblock copolymer micelle/DNA assembly is surrounded by an outermost polymer layer predominantly composed of the PEG chains. For simplicity we refer to this type of DNA complex formed with polymer micelles hereafter as “micelleplexes”, which is in analogy to other previously identified structures termed “polyplexes” or “lipoplexes”. We then present discussions of various properties of the micelleplexes that are important for potential gene delivery applications: (i) the size, charge and morphological characteristics, (ii) the stability against aggregation under physiologically relevant conditions, (iii) the relative binding affinity between the micelle and DNA, (iv) the ability to protect DNA against enzymatic degradation, and (v) the gene transfection efficiency and cytotoxicity in mammalian cells. These properties are discussed in comparison with those of the PDMAEMA homopolymer and PEG-PDMAEMA diblock copolymer-based polyplexes to elucidate the effects of the presence of the hydrophobic PnBA component on the properties and performances of the polymer-DNA complexes.

2. Experimental Procedures

2.1 Materials

The PEG-PnBA-PDMAEMA triblock copolymer, the PEG-PDMAEMA diblock copolymer and the PDMAEMA homopolymer used in this study were synthesized by atom transfer radical polymerization (ATRP) as described in Reference 38. The chemical structures and molecular characteristics of these polymers are shown in Table 1. Plasmid DNA Green Lantern-1 (pGL-1) which contains the green fluorescent protein (GFP) reporter gene and thus does not require a substrate for fluorescence detection was purchased from Gibco BRL. The plasmid was amplified in competent DH5α *Escherichia coli* (*E. coli*) and purified using a cesium chloride (CsCl) gradient ($OD_{260}/OD_{280} > 1.8$). Tris-HCl buffer (1.0 M, pH 7.5) was purchased from Invitrogen and diluted to 10 mM concentration with deionized water for subsequent use. DNase I (lyophilized powder), glycerol (molecular biology grade) and ethylenediaminetetraacetate (EDTA) solution (1.0 M, pH 8.0) were purchased from USB Corporation. Poly(aspartic acid) (PAA, $M_w=5000$ g/mol), ethidium bromide (EtBr, molecular biology grade) and sodium dodecyl sulfate (SDS, 99% purity) were purchased from Sigma-Aldrich. Polaroid 667 films (for real time imaging of gel electrophoresis images) were purchased from VWR Scientific.

2.2 Micelleplex/Polyplex Preparation and Characterization

PEG-PnBA-PDMAEMA micelles—PEG-PnBA-PDMAEMA micelles were prepared using the solvent exchange method as follows. A 1.0 % (w/v) solution of PEG-PnBA-PDMAEMA in DMF was prepared and transferred to a dialysis bag (molecular weight cut-off 3.5 kDa) which was then placed in 10 mM Tris-HCl buffer (pH 7.5, Invitrogen). Solvent exchange across the dialysis membrane was continued for 72 hours under constant stirring of the buffer solution. In the meantime, the solution was replaced with a fresh buffer every 24 hours. Consequently, we obtained a 0.41 % (w/w) micelle solution in the aqueous buffer.

Micelleplexes/polyplexes—Separate stock solutions of pGL-1, the PEG-PnBA-PDMAEMA micelles, PEG-PDMAEMA and PDMAEMA were prepared in 10 mM Tris-HCl buffer (pH 7.5) at respective concentrations of [pGL-1] = 0.500 mg/ml (which gives $[PO_4^{3-}] = 1.52 \mu\text{mol}/\text{ml}$), [PEG-PnBA-PDMAEMA] = 0.391 mg/ml ([amine] = 1.52 $\mu\text{mol}/\text{ml}$), [PEG-PDMAEMA] = 0.295 mg/ml ([amine] = 1.52 $\mu\text{mol}/\text{ml}$) and [PDMAEMA] = 0.238 mg/ml ([amine] = 1.52 $\mu\text{mol}/\text{ml}$). To prepare micelleplex/polyplex solutions at desired N:P ratios (defined as the ratio of the number of positive amine (N) groups on PDMAEMA to the number of negative phosphate (P) groups on pGL-1), appropriate amounts of micelle/polymer stock solutions were added to 200 μl pGL-1 stock solutions, and immediately after the mixing of the above components, the mixtures were agitated vigorously for 2 minutes. Subsequently, the volumes were adjusted to 2.0 ml ([pGL-1] = 50 $\mu\text{g}/\text{ml}$ in the final state) by adding suitable amounts of 10 mM Tris-HCl buffer solution, and the suspensions stirred for another 30 minutes. Thereafter, these micelleplex/polyplex solutions were stored quiescently at room temperature.

Electrophoretic mobility shift assays—Micelleplex and polyplex solutions were prepared at seven different N:P ratios: i.e., N:P = 0.5, 1, 2, 3, 5, 7 and 9. For each sample, an aliquot of 20 μl was mixed with 5 μl loading buffer (containing EtBr, Sigma-Aldrich), and this mixture was loaded into each sample well of a 1% (w/w) electrophoresis-grade agarose (VWR) gel. Electrophoresis was performed for 2 hours at 84 V in Tris-acetate-EDTA buffer. After destaining the gel for 5 hours in DI water (to eliminate background fluorescence), fluorescence images of the gel were recorded on Polaroid 667 film.

Particle size and ζ -potential measurements—The mean hydrodynamic diameters and ζ -potentials of the micelle, micelleplex and polyplex particles dispersed in the buffer solution were measured by dynamic light scattering (DLS) and phase angle light scattering (PALS), respectively, according to the procedures described in the Experimental Procedures section of the Supporting Information (SI).

Cryo-TEM—Thin liquid film specimens were prepared from 3 – 4 μl aliquots of a triblock micelle solution (prepared at a polymer concentration of 0.27 mg/ml) and the micelleplex solution (prepared as described in the previous paragraph) on holey TEM grids (R2/2, Quantifoil Micro Tools GmbH, Germany) and vitrified with liquid ethane at its melting temperature using a guillotine style plunging device.³⁹ Imaging was performed with an FEI Electron CM200 FEG microscope (200 kV). Appropriate underfocus (e.g., – 3.9 μm at a nominal magnification of 88,000 \times) was used for contrast enhancement. Images were digitally recorded on a Gatan CCD camera and processed using DigitalMicrograph software.

$^1\text{H NMR}$ —Tris base (1.09 g, 9.00 mmol, USB Corporation) was dissolved in 900 ml D₂O (98+ atom% D), and pH was adjusted to 7.46 by adding 810 μl of concentrated HCl. The resultant 10 mM deuterated Tris-HCl buffer was used as solvent for the NMR measurements on the micelle and micelleplex samples. Using the same solvent exchange procedures described earlier (i.e., via dialysis of a 1.0 % (w/v) solution of PEG-PnBA-PDMAEMA in

2.6 ml DMF against 300×3 ml of the deuterated Tris-HCl buffer for 72 hours), a 0.29% (w/w) PEG-PnBA-PDMAEMA micelle solution in the deuterated buffer was initially prepared. This micelle solution was then concentrated to a final concentration of 0.83% (w/w) by slow drying prior to the NMR experiment. Using stock solutions of pGL-1 (0.50 mg/ml) and the triblock copolymer micelles (0.391 mg/ml), a 2.0 ml micelleplex suspension at 7:1 N:P ratio was prepared according to the procedure described earlier. This suspension was concentrated by evaporating D₂O under weak vacuum to a final volume of 0.60 ml before taking the NMR spectra.

Salt and serum albumin-induced aggregation assays—The micelleplex and polyplex solutions were prepared at N:P = 7 as described above and homogenized immediately prior to these experiments. For examination of the aggregation properties of the micelleplex/polyplex particles under physiological salt concentration (150 mM), 1.8 ml of the micelleplex/polyplex solution was transferred to a dust-free polystyrene cuvette and equilibrated at 25 °C inside the ZetaPALS instrument for 10 minutes. Then, 187 µl of 1.5 M phosphate buffered saline (PBS) was added to this solution, and the mean hydrodynamic diameter of the polymer-DNA complexes was measured by DLS at a regular time interval for 1 hour. The aggregation properties of the micelleplex/polyplex particles in the presence of bovine serum albumin (BSA, Sigma-Aldrich) were measured by DLS in a similar fashion; first, 1.6 ml of the micelleplex/polyplex solution was equilibrated at 25 °C inside the ZetaPALS instrument for 10 minutes; afterwards, 400 µl of 0.20 g/ml BSA solution in 10 mM Tris-HCl buffer was added to it, and the mean hydrodynamic diameter of the complex particles was measured at a regular time interval for 1 hour.

Erythrocyte aggregation assays—A suspension of erythrocytes from the whole blood of calves (10% by volume) was purchased from Rockland Immunochemicals, Inc. The sample was diluted, immediately prior to these experiments, to a concentration of 0.1% (v/v) using calcium and magnesium-free saline (CMF). 200 µl of this erythrocyte suspension was loaded into each well of a 24-well plate (Falcon), and subsequently, 100 µl of the micelleplex/polyplex solution (prepared at N:P = 7) was added into it. The plate was incubated at room temperature for 3 hours under constant agitation. At a regular time interval, bright-field images of the erythrocyte cells were recorded using a Leica inverted fluorescence microscope (at 40× magnification) equipped with a Retiga 2000R Fast camera and the QCapture Pro software (QImaging Corporation).

DNA degradation assays—A DNase I stock solution was first prepared by dissolving DNase I powder in a 1:1 (by weight) mixture of glycerol and 1 mM CaCl₂ solution in DI water at a DNase I concentration of 0.01066 U/µl, and stored at -20°C before use. A typical pGL-1 degradation reaction was carried out at room temperature by mixing 160 µl of a micelleplex (or polyplex) solution (containing 50 µg/ml pGL-1 in 10 mM Tris-HCl buffer at an N:P of 7:1) with 2 µl of the DNase I solution and 40 µl of 50 mM MgSO₄·7H₂O solution prepared in 10 mM Tris-HCl buffer. The reaction mixture was constantly shaken during the reaction period, and aliquots (25 µl) of the sample were collected at desired time intervals. Immediately after the collection, each time sample was treated with 2.5 µl of the 1.0 M EDTA solution (for inactivation of DNase I). Subsequently, 5 µl of 8.0 mg/ml PAA solution prepared in 10 mM Tris-HCl buffer was added to the sample, and the mixture was incubated at room temperature for 24 hours under constant shaking to dissociate the DNA from the micelleplex (or polyplex) structure prior to the gel electrophoresis experiment. For gel electrophoresis analysis, the dissociated solution was mixed with 5.5 µl loading buffer, and this mixture (38 µl) was loaded into 1% (w/w) solution of agarose gel containing 0.5 µg/ml EtBr. The electrophoresis was conducted in 1× Tris-acetate-EDTA buffer for 2 hours at 84

V. The gel was then destained for minimum 28 hours with DI water (to remove excess EtBr) and imaged using the Polaroid film recorder.

Poly(aspartic acid)(PAA)-induced DNA unbinding assays—PAA solutions in 10 mM Tris-HCl buffer were prepared at seven different PAA concentrations of 0.2, 0.4, 0.6, 0.8, 1.0, 2.0, and 4.0 mg/ml. 10 μ l of these solutions were added to seven different 20 μ l micelleplex (or polyplex) solutions containing 50 μ g/ml pGL-1 at an N:P ratio of 7:1. The mixtures were initially vigorously agitated and then incubated at room temperature for 24 hours under constant shaking to induce dissociation of the micelleplex (or polyplex). Afterwards, each sample (containing 1 μ g of pGL-1) was mixed with 5 μ l of a gel electrophoresis loading buffer, and these mixtures (each 35 μ l in volume) were loaded into 1.0% (w/w) agarose gel containing 0.5 μ g/ml EtBr. Pristine pGL-1 was used to generate a marker signal corresponding to the completely dissociated state of the DNA-micelle (or DNA-polymer) complex. The samples were electrophoresed in 1 \times Tris-acetate-EDTA buffer for 2 hours at 84 V. The gel was then destained for 21 hours with DI water and photographed using a Polaroid 667 film system.

2.3 In Vitro Performance Assays

Reporter gene transfection assays—HeLa cells were seeded on 60-mm plates (Falcon) at a density of 4×10^5 cells per plate, and grown at 37 °C under 5% CO₂ atmosphere in 3 ml growth medium (Dulbecco's Modified Eagle Medium (DMEM)) containing 10% fetal bovine serum (FBS) and 1% penicillin/streptomycin. Twenty four hours after the seeding, the medium was replaced with fresh growth medium, and then 100 μ l per plate of the micelleplex/polyplex solution (containing 5 μ g pGL-1) was added to the cells. After 4 hours of incubation (to allow sufficient uptake of the complexes by the cells), the medium was aspirated off, and fresh growth medium (with no DNA particles in it) was added to the cells. The cells were grown for another 24 hours (to allow time for expression of GFP), and then the medium was removed. The cells were then trypsinized and fixed in 1 ml of 4% formalin solution in neutral buffered saline for 15 minutes at room temperature. The fixed cells were washed thrice with 1 \times PBS to remove excess paraformaldehyde and finally suspended in 0.5 ml 1 \times PBS. The cell suspensions were stored at 4 °C in dark prior to the measurements of the gene transfection efficiencies by flow cytometry. Flow cytometry analyses were performed on a Cytomics™ FC500 cytometer (Beckman-Coulter). A 488-nm air-cooled argon laser was used to excite GFP, and the emitted light was filtered by a 525-nm band-pass filter. The cells were gated by forward and side-scatter parameters, and data were collected from a population of 20,000 gated cells. The data were analyzed using the Cytomics FC500 RXP software.

Cytotoxicity assays—HeLa cells were seeded on 60-mm plates at a density of 4×10^5 cells per plate, and transfected with the micelleplexes/polyplexes using the same procedures as described above, except that for cytotoxicity assays, the cells were transfected for 24 hours. After the transfection, the medium was aspirated off, and fresh growth medium was added. After another 24 hours of incubation, the viabilities of the cells were measured by the standard MTT (methylthiazol tetrazolium) assay; see the SI for details of the procedures.

3. Results and Discussion

3.1 Size, Charge and Morphological Characteristics of the Micelle-like Aggregates formed by the PEG-PnBA-PDMAEMA Triblock Copolymer—

Because of the large size of the hydrophobic block, the PEG-PnBA-PDMAEMA triblock copolymer does not readily dissolve in water to form a micelle solution when it was simply placed and stirred in water. Thus, to prepare micelles of this triblock copolymer, the polymer was first dissolved in *N,N*-dimethylformamide (DMF), a common solvent for all three

component polymers, and then the micellar aggregation was induced by replacement of the initial solvent with 10 mM Tris-HCl buffer (pH 7.5) via a dialysis process. The structures of the micellar aggregates thus prepared were examined using cryo-TEM, and a representative cryo-TEM image is shown in Figure 1. As can be seen from the image, under typical cryo-TEM imaging conditions only the hydrophobic cores of the micelles were visible as distinct entities; the corona layer in which the hydrated PEG and PDMAEMA chains are situated was not visualizable. From analysis of cryo-TEM images, the average diameter of the hydrophobic core is estimated to be 19 ± 5 nm, indicating the formation of uniformly sized micelle-like aggregates by the PEG-PnBA-PDMAEMA copolymer in the buffer solution. Using this value of the micelle core diameter and also the molecular weights of the individual blocks of the triblock copolymer (estimated from the NMR data), it can be estimated that, on average, each micelle contains about 173 PEG chains and 173 PDMAEMA chains in the corona. The hydrodynamic diameter of the triblock copolymer micelles was measured by DLS to be 50 ± 18 nm, suggesting a mean thickness of the corona layer of approximately 15 nm.

For electrostatic complexation with DNA, it is essential for the PDMAEMA chains in the micelle corona to possess positive charges. In the Tris-HCl buffer (pH 7.5), the zeta potential of the micelle was measured to be highly positive (25.7 ± 0.2 mV), confirming that the PDMAEMA corona chains are positively charged because of the protonation of the tertiary amine groups under the given pH. The charged PDMAEMA segments in the micelle corona serve as binding sites when the micelle is exposed to negatively charged DNA.

3.2 Size, Charge and Morphological Characteristics of the Micelleplexes

Using the pGL-1 plasmid DNA, we confirmed that simply mixing the triblock copolymer micelles with DNA in aqueous buffer solution produces electrostatic complexes between DNA and the triblock copolymer micelle (i.e., micelleplexes) that have well-defined and reproducible nanostructures and charge characteristics. We prepared micelleplex samples at seven different N:P ratios ranging from 0.5 to 9; each sample was prepared by adding a prescribed amount of micelles dispersed in 10 mM Tris-HCl buffer (pH 7.5) to a separately prepared DNA solution in the same buffer to a desired final N:P ratio and a final pGL-1 concentration of 50 μ g/ml. We then examined the gel electrophoretic migration patterns of the complexed DNA for these micelleplex samples, and the results are presented in Figure 2(A). Also shown as reference in Figure 2(A) is the electrophoretic data of the uncomplexed plasmid DNA which display two distinct electrophoretic bands; the higher and lower-mobility bands respectively correspond to the supercoiled and relaxed circular forms of the plasmid. In the cases involving the micelle-complexed DNA at low N:P ratios (= 0.5 and 1), broad smears typically appear between the positions of the loading well and the naked DNA bands, indicating heterogeneous sizes and/or structures of the micelle/DNA complexes under these relatively low N:P conditions. With increasing N:P ratio, this smear gradually shifts to the loading position, and at N:P equal to 3 or higher, the complexed DNA loses its ability to migrate through the gel and becomes confined within the loading hole. As will be discussed later in this subsection, at N:P ratios greater than 3, the micelleplexes assume net positive charges. It is of note that, however, this positive charge does not cause the high-N:P micelleplexes to migrate toward the opposite (negative) electrode under the electrophoresis condition, which is believed to be due to the compact structures and the relatively large sizes of the micelleplexes (as will also be discussed in detail later). For comparison, identical electrophoretic mobility assays were performed with simple PDMAEMA-based polyplexes, and also with PEGylated polyplexes prepared using the PEG-PDMAEMA diblock copolymer, under the same set of N:P conditions as used in the micelleplex experiments. As shown in Figures 2(B) and 2(C), the polyplex analogues exhibit comparable electrophoretic migration patterns as functions of the N:P ratio. It is of note, in Figures 2(A) through 2(C),

that the intensity of the DNA band at the loading position shows an interesting dependence on the N:P ratio, and the observed behaviors can likely be explained in terms of the combined effects of the following factors: the fraction of DNA complexed to the polycation segments, the strength of the binding between the DNA and the polycation charges, and the inter-polyplex/micelleplex aggregation.⁴⁰

The detailed dependences of the micelleplex size and charge characteristics on the N:P ratio were investigated using the combined DLS and PALS ζ -potential measurement techniques. As shown in Figure 3, at N:P = 0.5, the micelleplex still shows a negative ζ -potential. With the increase of the N:P ratio, the micelleplex ζ -potential increases, and it becomes electroneutral at an N:P of about 3. These results are consistent with the gel electrophoresis data. Further increase of the N:P value causes an overcompensation of the DNA charge by the triblock copolymer micelles, similarly to what has been commonly observed in simple polyplex systems⁹. We observe that both the size and ζ -potential of the micelleplexes level off at an N:P ratio of about 5. As compared in Figure 3, the PEGylated polyplex system exhibits qualitatively similar trends in the N:P dependences of their size and charge properties. In the simple (non-PEGylated) polyplex case, however, at N:P ratios close to the zero net charge condition (i.e., $1 < \text{N:P} < 5$), both the size and charge values become unmeasurably large, because of the agglomeration of the polyplex particles that occurs due to the absence of the electrostatic repulsion between the particles. We note that in all three cases, the size and charge properties become relatively independent of the N:P parameter at around N:P = 7, and in the studies presented in the remaining sections of this article, we used this N:P value to investigate the detailed structural properties of the micelleplexes (in the remainder of this section and Section 3.3) and also to compare their stability properties with their polyplex equivalents (Sections 3.4 through 3.7).

As shown in Figure 3, the micelleplexes are typically larger than the PEGylated polyplexes under identical N:P conditions; for instance, at N:P = 7, the average hydrodynamic diameters of the micelleplex and the PEGylated polyplex are 211 ± 20 and 149 ± 1 nm, respectively. This difference is believed to be associated with the difference in the building block size between the micelleplex and PEGylated polyplex cases (i.e., the triblock copolymer micelle vs. the PEG-PDMAEMA copolymer). Both of these complex types provide DNA particle sizes that are smaller than the smallest capillaries in the body⁴¹, and are also appropriate for cellular uptake⁴²; data confirming high levels of cellular uptake of the polyplex/micelleplex particles are provided in Figure S1 of the SI. As discussed in Section 3.3, the micelleplex assembly is coated with an outer layer of the PEG chains, and for this reason, the micelleplex structure is stable against aggregation over a long period of time; using DLS, we confirmed that the size of the micelleplex (at N:P = 7) remained unchanged for over 3 months after preparation (data not shown). The PEGylated polyplex system at the same N:P condition also exhibited similar stability over the same measurement period (data not shown). However, the simple PDMAEMA-based polyplexes (at N:P = 7) formed macroscopic agglomerates over a relatively short time (2 – 3 days) despite its positive surface charge ($\zeta = 30.0 \pm 0.8$ mV). In fact, at all N:P ratios studied (Figure 3), the sizes of the PDMAEMA polyplexes (measured within 30 minutes of preparation) were measured to be larger than both the micelleplex and PEG-PDMAEMA polyplex systems, suggesting that in the simple polyplex case, the agglomeration occurs even during the course of preparation of the polyplexes. This is also supported by the observation that the size of the homopolymer polyplex is dependent upon the DNA and PDMAEMA concentrations; for example, at a fixed N:P of 7, the mean hydrodynamic diameters of the PDMAEMA-based polyplexes prepared at two different DNA concentrations of 5 and 10 $\mu\text{g}/\text{ml}$ were measured to be 124 ± 68 and 216 ± 63 nm, respectively. It is important to note that in the micelleplex case (and also in the PEGylated polyplex case), the complexes sizes were found to be

insensitive to the same change in the DNA and micelle (or PEG-PDMAEMA) concentrations under the high N:P conditions (e.g., N:P = 7:1).

The detailed structures of the micelleplexes were examined using cryo-TEM. Figure 4 presents a representative image taken from a micelleplex solution containing 50 µg/ml pGL-1 in the Tris-HCl buffer (10 mM, pH 7.5) at an N:P ratio of 7:1. As shown in the figure, the complexation of DNA with the PDMAEMA chains in the micelle corona results in condensation of the DNA molecules into compact structures such as multi-molecular rod-like bundles, toroids or spherical globules. The basic morphologies that are observed in these systems are similar to those previously reported for DNA condensates derived using homopolymer⁴³ or PEG-modified⁴⁴ polycations. Unlike many cases involving simple polyplexes, however, the micelleplexes generally exhibit pronounced heterogeneities in their morphologies, and thus it is reasonable to expect that these observed morphologies are kinetically frozen (non-equilibrium) structures that arise from strong electrostatic interactions and slow kinetics associated with the large sizes of the building block components (i.e., the micelles). Assuming that in the bundle-like structure, the condensed DNA strands are aligned in a hexagonal arrangement with a typical center-to-center separation distance of about 3 nm between two adjacent double-stranded DNA helices,⁴⁵ and using structural parameter values estimated from the cryo-TEM image (i.e., a bundle diameter of 31.7 ± 3.4 nm, and an estimate of 170 ± 42 for the number of adsorbed micelles per µm of bundle length), we estimate an average N:P ratio of 7(±2):1 for a typical bundled region in the micelleplex, which compares favorably with the bulk N:P ratio of 7:1 calculated using the total concentrations of the amine and phosphate groups in the system. For this reason, and considering that we have not detected any unbound micelles that stay free in the aqueous phase, we believe that the observed local structures of the micelleplexes reasonably represent the overall micelleplex population. Also, of note in Figure 4 is that the PnBA micelle cores are quite uniformly spaced from one another on the micelleplex surface, which reflects the presence of a strong (steric) repulsion between neighboring micelles caused by the overlapping of the PEG brush layers in the inter-micelle interstices, and therefore indicates that the encapsulated portions of the DNA molecules are completely shielded by the micellar coat.

3.3 The outer surface of the micelleplex is predominantly coated with the PEG chains

It is known that condensation of DNA by multivalent cations generally involves neutralization of approximately 80 – 90% of the negative charges on the DNA molecules.⁴⁶ Assuming a similar behavior in our system, we expect that in the micelleplexes prepared, for instance at an N:P ratio of 7:1, only about 11 – 13% of the amine groups on the PDMAEMA chains participate directly in the charge neutralization process. Therefore, it is not automatically clear that when the micelles are bound to condensed DNA, all of the PDMAEMA chains in the micelle corona spontaneously orientate towards the inner domain of the micelleplex, and only the non-charged (bioinert) PEG chains remain present at the outer surface of the micelleplex; such a feature would indeed make the micelleplex structure potentially useful for biomedical delivery applications. Evidence that supports this brush rearrangement scenario was obtained from ¹H NMR spectroscopy experiments. We performed ¹H NMR measurements on the triblock copolymer micelles dispersed in D₂O both in the presence and absence of pGL-1 DNA. As displayed in Figure 5(B), the NMR spectra obtained from a 0.91 mg/ml micelle solution (in 10 mM deuterated Tris-HCl buffer) with no DNA present exhibited all the resonances corresponding to the protons on the PEG (i.e., at 3.6 ppm) and PDMAEMA (0.9–1.1, 1.8–1.9, 2.3, 2.6 and 4.1 ppm) chains. The PnBA chains, on the other hand, form the hydrophobic core domains of the micelles in which the mobility of the constituent chains is significantly restricted. For this reason, the micellization results in (broadening and) virtual disappearance of the PnBA signals which

would otherwise appear at distinct chemical shifts (e.g., $\delta = 1.4$ and 1.6 ppm in CDCl_3 , as demonstrated in Figure S2 in SI). The sharpness of the PEG and PDMAEMA peaks in Figure 5(B) is essentially the same as that observed with the triblock copolymer in its molecularly dissolved state in a common solvent (i.e., CDCl_3) (Figure S2), confirming the existence of highly hydrated (mobile) PEG and PDMAEMA segments in the corona of the micelles. However, the effective area ratio between the PDMAEMA and PEG peaks in Figure 5(B) is measured to be about 30% of that calculated on the basis of the molecular compositions of the constituent block copolymers, which indicates that, after the micellization, a significant fraction (i.e., about 70%) of the PDMAEMA segments become incorporated into the hydrophobic core domain. Figure 5(C) presents the NMR data for the triblock copolymer micelles complexed with pGL-1 DNA at an N:P ratio of 7:1 (with a final DNA concentration of $50\ \mu\text{g}/\text{ml}$ in the deuterated Tris-HCl buffer). The size and sharpness of the peaks corresponding to the protons of the PEG segments remain unaffected by the complexation of the micelles with DNA molecules. However, the peaks associated with the cationic PDMAEMA chains show a significant broadening and (about 88%) reduction in the effective area after micelleplex formation, which indicates that the complexation causes a loss of mobility in the majority of the PDMAEMA chains in the system, while it has no influence on the PEG brushes. The NMR results corroborate that binding of the micelles to DNA involves a conformational rearrangement and segregation of the PDMAEMA and PEG chains in the micelle corona; that is, the PDMAEMA chains become bound to the condensed DNA, and the PEG chains form the outermost brush layer surrounding the whole micelleplex assembly (as depicted schematically in Figure 5(D)). The chemical sequence and connectivity of the component blocks in the PEG-PnBA-PDMAEMA triblock copolymer causes the hydrophobic micelle cores to be located in a monolayer arrangement between the PEG-rich outer layer and the PDMAEMA-rich inner domain of the micelleplex.

3.4 Stability of the Micelleplexes/Polyplexes against Aggregation under Physiologically Relevant Conditions

The effects of the polymer chemistry on the stability of the polymer-DNA complexes against aggregation were examined under three different conditions: i.e., (a) under physiological salt concentration ($150\ \text{mM}\ \text{NaCl}$), (b) in the presence of serum albumin, and (c) in the presence of erythrocytes; these are three of the major components of the blood that are typically responsible for the aggregation of DNA polyplexes. Figure 6 presents plots summarizing the aggregation behaviors of the three different DNA complexes under $150\ \text{mM}\ \text{NaCl}$. For this study, $187\ \mu\text{l}$ of $1.5\ \text{M}\ \text{PBS}$ to a $1.8\ \text{ml}$ solution of each type of DNA complex (prepared at N:P = 7 in $10\ \text{mM}\ \text{Tris-HCl}$ buffer (pH 7.5)), and the average hydrodynamic diameter of the complex particles was measured by DLS as a function of time for one hour. As shown in the figure, the simple PDMAEMA/DNA polyplexes start forming aggregates almost immediately (within the first few minutes) after the addition of PBS, and the aggregation behavior becomes stabilized at a diameter of approximately $1.66\ \mu\text{m}$ after about 40 minutes; it should be noted that at the given N:P ratio, without added salt, the PDMAEMA polyplexes are stable in $10\ \text{mM}\ \text{Tris-HCl}$ over this length of time. In both the PEG-PDMAEMA polyplex and micelleplex cases, no change in the size of the DNA particles was observed over the entire one-hour period.

Albumin constitutes the largest fraction of proteins in blood plasma,⁴⁷ and is normally negatively charged, causing the net positively-charged DNA complexes to be attracted to it.²⁰ We examined how the presence of albumin (at a physiological concentration of $40\ \text{mg}/\text{ml}$ ⁴⁷) influences the stabilities of the micelleplexes/polyplexes; the sizes of the three different polymer-DNA complexes were monitored by DLS for 60 minutes after the addition of BSA into the respective solutions. As shown in Figure 6, the measured diameter of the PDMAEMA-DNA polyplexes shows an increase from 389 to $505\ \text{nm}$ within 12 minutes

upon addition of BSA, and becomes stable afterwards. No sign of BSA-induced aggregation was detected during the one-hour measurement period in both the PEGylated polyplex and micelleplex systems. These results are especially consistent with the fact that the exterior surface of the micelleplex structure is completely coated with a PEG brush layer (Section 3.3).

To test how the micelleplexes/polyplexes interact with erythrocytes (red blood cells), the micelleplexes/polyplexes prepared at N:P = 7 were mixed with bovine erythrocytes to final DNA and erythrocyte concentrations of 17 µg/ml and 0.067% (v/v), respectively, and the mixtures were imaged using light microscopy as a function of time. Representative bright-field images demonstrating how the aggregation of the erythrocyte cells induced by the presence of the PDMAEMA polyplexes progresses with time over a three-hour period are presented in Figure S3 of the SI; at about 2 hours after the mixing, the aggregation reaches a plateau level. Figure 7 compares the levels of aggregation of erythrocytes in the absence and presence of the three different DNA complexes after two hours of incubation with the respective complexes. With no added polymer-DNA complexes, erythrocytes are stable in CMF saline over the measured time scale. The PDMAEMA-based polyplexes induces the highest level of erythrocyte aggregation. In the presence of the PEG-PDMAEMA polyplexes or micelleplexes, erythrocytes remain largely unaggregated after the two hours, with only a small population of the cells existing in the aggregated state, confirming the PEG-coated structures of these polymer-DNA complexes. The erythrocyte clusters are slightly larger in size in the micelleplex case than with the PEG-PDMAEMA polyplexes.

3.5 Relative Binding Affinity between the Polymers and DNA

We examined the stability of the micelleplexes/polyplexes against the addition of a polyanion, such as poly(aspartic acid) (PAA), which competes with DNA for binding to the cationic polymer and causes dissociation of the original polycation/DNA binding.⁴⁸ Specifically, the PAA additive was added to seven identical micelleplex (or polyplex) solutions containing 50 µg/ml pGL-1 in the Tris-HCl buffer (at an N:P ratio of 7) to seven different final PAA concentrations (i.e., to final aspartic acid-to-phosphate (A:P) stoichiometric ratios of 5, 10, 15, 20, 25, 50 and 100). These mixtures were then incubated as described in the experimental section. Afterwards, the gel electrophoretic mobilities of the DNA molecules in these samples were examined. The results are presented in Figure 8. In the micelleplex system (Figure 8(A)), in the A:P range of 5 to 25, a major fraction of DNA molecules remain undissociated in the micelleplexes, giving rise to a strong band at the loading well. In this A:P regime, the addition of PAA to the micelleplexes appears to involve complicated patterns of dissociation behavior, and the occurrence of smear DNA bands indicates that the presence of PAA causes predominantly partial dissociation of the micelleplexes into smaller complexes with a distribution in their sizes and/or compositions. The degree of DNA dissociation is an increasing function of PAA concentration, as seen by the increasing smear of the micelleplex band towards lower molecular weight with the A:P ratio. At higher A:P ratios studied (i.e., A:P = 50 and 100), all the DNA molecules become completely dissociated from the micelleplexes into either supercoiled or circular plasmid DNA, as evidenced by the disappearance of the original micelleplex band at the loading position. In the PEGylated case (Figure 8(B)), sharp bands of the released DNA start appearing at a significantly lower A:P ratio (= 15), and at A:P = 50 or higher, the addition of PAA induces complete release of pGL-1 from the complexes, similarly to the dissociation of the micelleplexes. These trends observed between the two systems indicate that the binding affinity of the triblock copolymer micelles to DNA is stronger than that of its molecular analogues (i.e., the PEG-PDMAEMA diblock copolymer). These results can be understood considering that in the micelleplex case, we use supramolecular assemblies (i.e., micelle-like aggregates), instead of individual macromolecules, as basic building blocks for creating

condensed DNA particles. To elucidate this point, we consider a case in which each triblock copolymer micelle contains N cationic chains in the corona. Treating the complexation as an adsorption phenomenon, the equilibrium constant for the micelle binding to condensed DNA (K_N) can be related to the free energy change associated with the adsorption of the micelle (ΔF_N) by $K_N \approx \exp(-\Delta F_N/k_B T)$ in the limit of complete neutralization of the DNA charges⁴⁹. If we simplistically assume that $\Delta F_N \approx N\Delta F_I$ where ΔF_I is the free energy of adsorption for the polycation chain in its isolated form, it is easy to see that the probability of a micelle dissociation (P_{-N}), which can be given as $P_{-N} \approx 1/K_N$ in the strong adsorption limit, is significantly lower than that of the single polycation chain ($P_{-I} \approx 1/K_I \approx \exp(\Delta F_I/k_B T)$); i.e., $P_{-N} = (P_{-I})^N$. It should be noted that for large N , the linear relationship $\Delta F_N \approx N\Delta F_I$ loses its applicability, and the dependence of ΔF_N on N is expected to be much weaker⁵⁰, and therefore, the difference between P_{-N} and P_{-I} may not be that dramatic. Nonetheless, the argument remains a good guideline. It should be noted, however, that the data shown in Figure 8(C) indicate that the PDMAEMA homopolymer binds strongest to DNA among the three polyplex types tested; as shown in Figure 8(C), even at A:P = 50, a significant population of the PDMAEMA polyplexes continue to be in the undissociated state (unlike the other two cases discussed above). These results indicate that the presence of the PEG moiety weakens the binding between the polymer/micelle and DNA.

3.6 Ability of the Micelleplexes/Polyplexes to Protect DNA from Enzymatic Degradation

It is known in the literature that the binding stability of the DNA/polycation complex directly correlates to the ability of the complex to protect the encapsulated DNA from degradation by nuclease enzymes²⁶; this DNA protection capability is an important property required for a DNA/polycation complex to be useful as a gene carrier for *in vivo* applications. To determine whether the triblock copolymer micelles can protect DNA from enzymatic degradation and also how this property of the micelleplex system compares with those of its polyplex analogues under identical conditions, we used DNase I, an endonuclease that catalyzes the degradation of DNA to di-, tri- and oligo-nucleotides, as a model enzyme. Specifically, the micelleplexes and polyplexes (prepared with 50 µg/ml pGL-1 at N:P = 7) were exposed to 0.02132 U of DNase I (final DNase I concentration in the solution = 0.107 U/ml which is comparable to the DNase I concentration in human blood, 0.356 ± 0.410 U/ml as reported in Ref. 51) for varying durations, and these samples were subsequently treated with EDTA (for deactivation of the enzyme) and then with PAA (A:P = 100) at room temperature for an extended period of time (≈ 24 hours) to ensure complete release of the DNA from the complex. The resultant DNA samples were examined using the gel electrophoresis technique. As shown in Figure 9(A), the unprotected pGL-1 becomes almost completely degraded after 15 minutes of exposure to DNase I; when exposed to the enzyme, the DNA became fragmented into smaller sequences of varying lengths which were distinguished from the original plasmids in the gel electrophoresis pattern owing to their higher mobility under an external electric field, and the fluorescence from these DNA fragments relative to the signals from the undegraded DNA molecules could be used as a qualitative measure of the extent of degradation of the DNA as a function of the exposure time. Also of note is that in Figure 9(A), the detailed patterns of the changes in the relative intensities of the DNA bands reveal interesting kinetic features of these degradation processes. For instance, the circular form of pGL-1 becomes completely degraded within 15 minutes after exposure to DNase I, as evidenced by the disappearance of the corresponding band, whereas some small fraction of the supercoiled pGL-1 molecules remain undegraded even after 5 hours of DNase I treatment. Also, the DNase I degradation produces an additional band in the gel electrophoresis pattern which appears between the positions of the two bands corresponding to the supercoiled and circular forms of the undegraded pGL-1 (shown as markers in the leftmost lane in Figure 9(A)). This new band is believed to correspond to linear DNA chains generated by enzymatic cleavage of both the

supercoiled and circular pGL-1 molecules, and subsequently, these linear molecules are further degraded into smaller fragments. As shown in Figures 9(B) through 9(D), in the micelle or polycation-complexed situations, the sequence of events that occur during the degradation processes are similar to those seen with the unprotected pGL-1 (Figure 9(A)). In the micelleplex and polyplex cases, however, the relative amounts of the fragmented DNA were much lower at all exposure times than observed in the unprotected experiments, indicating that the micelleplex and polyplex formulations are all capable of providing a reasonable protection of DNA from the DNase I digestion. A comparison of the time-dependent degradation profiles among the three different types of DNA complexes (Figures 9(B) through 9(D)) indicates that the triblock copolymer micelles provide a better protection of the plasmid DNA against DNase I-induced degradation than the PEG-PDMAEMA, while among the three materials, the best protection of DNA was achieved with the PDMAEMA homopolymer. We note that these results corroborate the strong link between the DNA-polycation binding strength and the resistance of the complexed DNA against enzymatic degradation suggested by other authors.²⁶

3.7 *In Vitro* Gene Transfection Efficiency and Cytotoxicity of the Micelleplexes/Polyplexes

The *in vitro* gene transfection efficiencies of the three different DNA carriers were measured in HeLa cells. For this purpose, the respective polymer-DNA complexes were prepared at an N:P ratio of 7 using the pGL-1 plasmid as the reporter gene which encodes for GFP. HeLa cells were incubated with the respective DNA complexes for uptake of the DNA for four hours. After another 24 hours of incubation, the GFP expression levels in the HeLa cells were analyzed using flow cytometry. Two parameters were measured: the fraction of cells expressing GFP (“transfection efficiency”), and the mean fluorescence intensity (per cell) from the GFP-expressing cell population. The results are presented in Figure 10. As shown in the figure, all three systems are capable of causing some levels of GFP expression in HeLa cells. The PEG-coated systems (i.e., the PEG-PDMAEMA polyplexes and the micelleplexes) exhibit lower transfection efficiencies than the PDMAEMA polyplexes, consistent with the results in the literature; the PEGylation is known to reduce the cellular internalization of the polymer-DNA complexes.²⁸ The transfection efficiency is also negatively affected by the presence of the hydrophobic segments in the micelleplex structure; the transfection efficiency of the micelleplexes is slightly lower than that of the PEG-PDMAEMA polyplexes, presumably because of the stronger binding affinity between the micelle and DNA than between the PEG-PDMAEMA diblock copolymer and DNA. The observed differences in the GFP expression level among the three different gene carriers are not due to differences in their cytotoxicities, as confirmed by MTT cell viability assay; as shown in Figure 10(B), there is no significant difference in the cellular toxicity among the three different polymer-DNA complexes.

4. Conclusion and Outlook

In this paper, we examine the influence of adding a hydrophobic segment (as a middle block) to the conventional PEG-polycation diblock copolymer structure on the physicochemical and (cell-level) biological properties of the corresponding polymer-DNA complexes. For this purpose, we use polymer-DNA complexes prepared using three different polymers having, respectively, the homopolymer, diblock and triblock structures (i.e., PDMAEMA, PEG-PDMAEMA and PEG-PnBA-PDMAEMA, respectively), and compare their properties in various aspects. Unlike the other polymers, the PEG-PnBA-PDMAEMA triblock copolymer forms micelle-like aggregates in aqueous media due to the presence of the water-insoluble PnBA block (Section 3.1). The resultant micelles have mixed PEG and PDMAEMA chains in the corona. The electrostatic complexation between the micelles and DNA molecules simultaneously induces condensation of the DNA

molecules and sequestration of the cationic brush chains toward the inner side of the micelle coating layer, and as a result, micellar PEG brush-stabilized, condensed DNA particles (referred to as “micelleplexes”) are achieved (Sections 3.2 and 3.3). This morphological feature provides for the micelleplexes the colloidal stability against the addition of NaCl, BSA and erythrocytes, which is comparable to (or in the erythrocyte case slightly less than) that of the PEG-PDMAEMA polyplexes (Section 3.4). In terms of both the prevention of the PAA-induced dissociation of the polymer-DNA complexes (Section 3.5) and the protection of the encapsulated DNA against DNase I-induced degradation (Section 3.6), the micelleplexes are better than the PEG-PDMAEMA polyplexes, but are not better than the PDMAEMA polyplexes. The micelleplexes exhibit a lower transfection efficiency than the other two complexes; the PDMAEMA polyplexes show the highest transfection efficiency (Section 3.7). The cytotoxicity levels are comparable among the three different systems (Section 3.7). These results suggest that the hydrophobic modification offers enhancement of the physicochemical properties of the PEG-polycation-based DNA carriers, in particular, in terms of the DNA protection against enzymatic degradation. However, this improvement involves a trade-off with the gene transfection efficiency. It is envisioned that the micelleplex morphology can be used as a convenient platform for incorporation of additional functions to the delivery system. Toward enhancement of target specificity, controlled biodegradability and optimized intracellular activity, for instance, other established chemistries^{52–56} can be readily incorporated into the triblock copolymer and micelle designs. In addition to this flexibility in synthetic design, the micelleplex structure provides a separate cargo space, namely, the hydrophobic core of the micelle which can be used for carriage of additional bioactive substances⁵⁷ or ‘helper’ molecules (e.g., fluorescent dye molecules for intracellular tracking, quantum dots for *in vivo* imaging, etc.).

Supplementary Material

Refer to Web version on PubMed Central for supplementary material.

Acknowledgments

The authors would like to thank the National Science Foundation (CBET-0828574), the 3M Company (Nontenured Faculty Award), the Showalter Trust and the Purdue Research Foundation for providing financial support of this research. RS is grateful for the Bilsland PhD Dissertation Fellowship from the Graduate School of Purdue University.

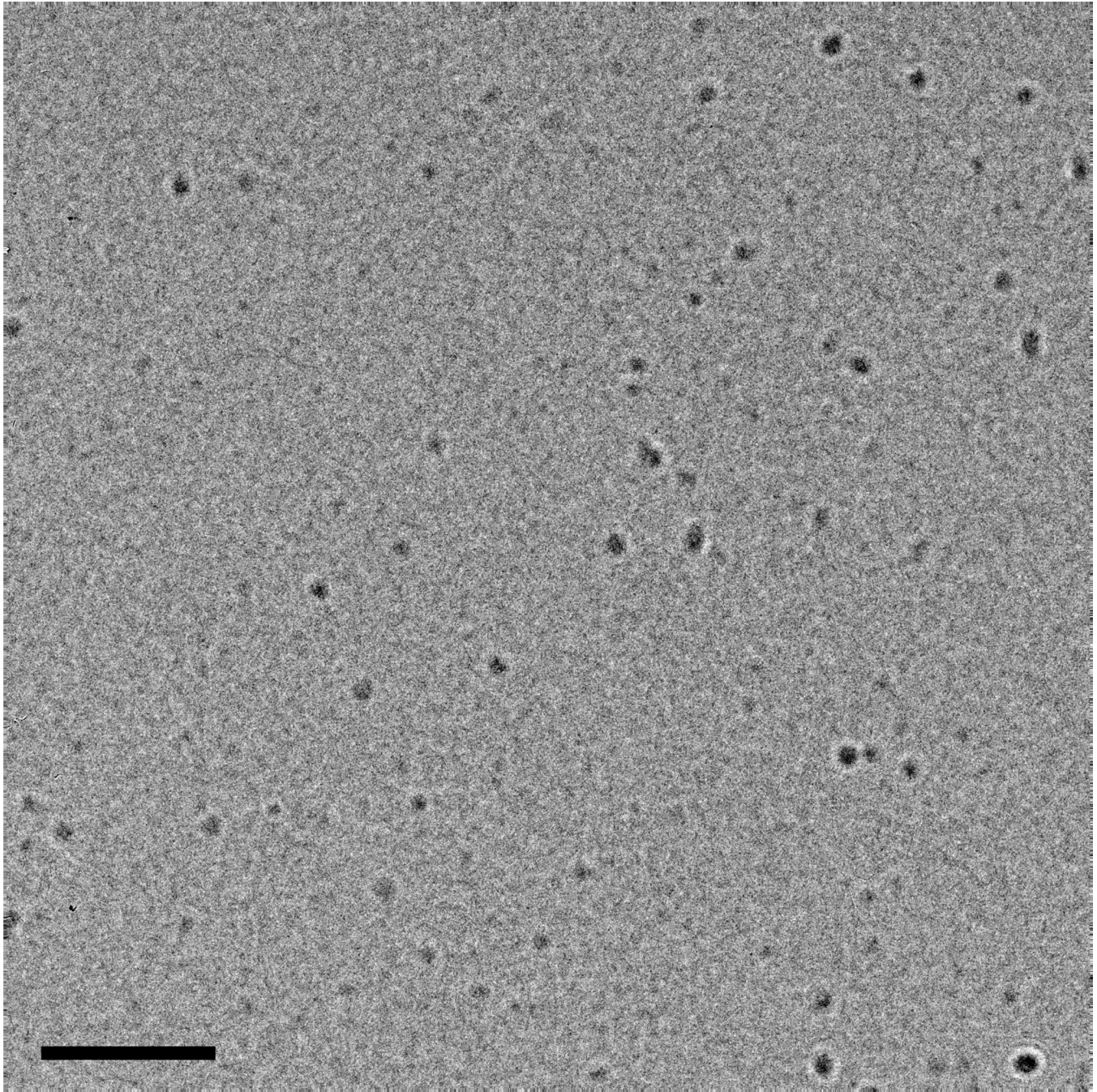
References and Notes

1. Anderson WF. Human Gene-Therapy. *Science*. 1992; 256(5058):808–813. [PubMed: 1589762]
2. Luo D, Saltzman WM. Synthetic DNA delivery systems. *Nat. Biotechnol.* 2000; 18(1):33–37. [PubMed: 10625387]
3. Davis ME. Non-viral gene delivery systems. *Curr. Opin. Biotechnol.* 2002; 13(2):128–131. [PubMed: 11950563]
4. Thomas CE, Ehrhardt A, Kay MA. Progress and problems with the use of viral vectors for gene therapy. *Nat. Rev. Genet.* 2003; 4(5):346–358. [PubMed: 12728277]
5. Wiethoff CM, Middaugh CR. Barriers to nonviral gene delivery. *J. Pharm. Sci.* 2003; 92(2):203–217. [PubMed: 12532370]
6. Putnam D. Polymers for gene delivery across length scales. *Nat. Mater.* 2006; 5(6):439–451. [PubMed: 16738681]
7. Leong KW. Polymeric controlled nucleic acid delivery. *MRS Bull.* 2005; 30(9):640–646.
8. Barthelemy P, Camplo M. Functional amphiphiles for gene delivery. *MRS Bull.* 2005; 30(9):647–653.
9. De Smedt SC, Demeester J, Hennink WE. Cationic polymer based gene delivery systems. *Pharm. Res.* 2000; 17(2):113–126. [PubMed: 10751024]

10. Park TG, Jeong JH, Kim SW. Current status of polymeric gene delivery systems. *Adv. Drug Deliv. Rev.* 2006; 58(4):467–486. [PubMed: 16781003]
11. Gebhart CL, Kabanov AV. Perspectives on polymeric gene delivery. *J. Bioact. Compat. Polym.* 2003; 18(2):147–166.
12. Lee M, Kim SW. Polyethylene glycol-conjugated copolymers for plasmid DNA delivery. *Pharm. Res.* 2005; 22(1):1–10. [PubMed: 15771224]
13. Boussif O, Lezoualch F, Zanta MA, Mergny MD, Scherman D, Demeneix B, Behr JP. A Versatile Vector for Gene and Oligonucleotide Transfer into Cells in Culture and in-Vivo - Polyethylenimine. *Proc. Natl. Acad. Sci. U. S. A.* 1995; 92(16):7297–7301. [PubMed: 7638184]
14. Liu G, Molas M, Grossmann GA, Pasumarthy M, Perales JC, Cooper MJ, Hanson RW. Biological properties of poly-L-lysine-DNA complexes generated by cooperative binding of the polycation. *J. Biol. Chem.* 2001; 276(37):34379–34387. [PubMed: 11438546]
15. van de Wetering P, Chering JY, Talsma H, Crommelin DJA, Hennink WE. 2-(dimethylamino)ethyl methacrylate based (co)polymers as gene transfer agents. *J. Control. Release.* 1998; 53(1–3):145–153. [PubMed: 9741922]
16. Tang MX, Redemann CT, Szoka FC. In vitro gene delivery by degraded polyamidoamine dendrimers. *Bioconjugate Chem.* 1996; 7(6):703–714.
17. Gonzalez H, Hwang SJ, Davis ME. New class of polymers for the delivery of macromolecular therapeutics. *Bioconjugate Chem.* 1999; 10(6):1068–1074.
18. Little SR, Lynn DM, Ge Q, Anderson DG, Puram SV, Chen JZ, Eisen HN, Langer R. Poly-beta amino ester-containing microparticles enhance the activity of nonviral genetic vaccines. *Proc. Natl. Acad. Sci. U. S. A.* 2004; 101(26):9534–9539. [PubMed: 15210954]
19. Lim YB, Kim SM, Lee Y, Lee WK, Yang TG, Lee MJ, Suh H, Park JS. Cationic hyperbranched poly(amino ester): A novel class of DNA condensing molecule with cationic surface, biodegradable three-dimensional structure, and tertiary amine groups in the interior. *J. Amer. Chem. Soc.* 2001; 123(10):2460–2461. [PubMed: 11456910]
20. Ogris M, Brunner S, Schuller S, Kircheis R, Wagner E. PEGylated DNA/transferrin-PEI complexes: reduced interaction with blood components, extended circulation in blood and potential for systemic gene delivery. *Gene Ther.* 1999; 6(4):595–605. [PubMed: 10476219]
21. Templeton NS, Lasic DD, Frederik PM, Strey HH, Roberts DD, Pavlakis GN. Improved DNA: Liposome complexes for increased systemic delivery and gene expression. *Nat. Biotechnol.* 1997; 15(7):647–652. [PubMed: 9219267]
22. Kakizawa Y, Kataoka K. Block copolymer micelles for delivery of gene and related compounds. *Adv. Drug Deliv. Rev.* 2002; 54(2):203–222. [PubMed: 11897146]
23. Hwang SJ, Davis ME. Cationic polymers for gene delivery: Designs for overcoming barriers to systemic administration. *Curr. Opin. Mol. Ther.* 2001; 3(2):183–191. [PubMed: 11338932]
24. Fischer D, Osburg B, Petersen H, Kissel T, Bickel U. Effect of poly(ethylene imine) molecular weight and pegylation on organ distribution and pharmacokinetics of polyplexes with oligodeoxynucleotides in mice. *Drug Metab. Dispos.* 2004; 32(9):983–992. [PubMed: 15319340]
25. Merdan T, Kunath K, Petersen H, Bakowsky U, Voigt KH, Kopecek J, Kissel T. PEGylation of poly(ethylene imine) affects stability of complexes with plasmid DNA under in vivo conditions in a dose-dependent manner after intravenous injection into mice. *Bioconjugate Chem.* 2005; 16(4): 785–792.
26. Mullen PM, Lollo CP, Phan QC, Amini A, Banaszczyk MG, Fabrycki JM, Wu DP, Carlo AT, Pezzoli P, Coffin CC, Carlo DJ. Strength of conjugate binding to plasmid DNA affects degradation rate and expression level in vivo. *Biochim. Biophys. Acta-Gen. Subj.* 2000; 1523(1): 103–110.
27. Harris, JM.; Zalipsky, S. *Poly(ethylene glycol): Chemistry and Biological Applications.* Washington: American Chemical Society; 1997.
28. Mishra S, Webster P, Davis ME. PEGylation significantly affects cellular uptake and intracellular trafficking of non-viral gene delivery particles. *Eur. J. Cell Biol.* 2004; 83(3):97–111. [PubMed: 15202568]
29. Gebhart CL, Kabanov AV. Evaluation of polyplexes as gene transfer agents. *J. Control. Release.* 2001; 73(2–3):401–416. [PubMed: 11516515]

30. Gebhart CL, Sriadibhatla S, Vinogradov S, Lemieux P, Alakhov V, Kabanov AV. Design and formulation of polyplexes based on pluronic-polyethyleneimine conjugates for gene transfer. *Bioconjugate Chem.* 2002; 13(5):937–944.
31. Alvarez-Lorenzo C, Barreiro-Iglesias R, Concheiro A, Iourtchenko L, Alakhov V, Bromberg L, Temchenko M, Deshmukh S, Hatton TA. Biophysical characterization of complexation of DNA with block copolymers of poly(2-dimethylaminoethyl) methacrylate, poly(ethylene oxide), and poly(propylene oxide). *Langmuir.* 2005; 21(11):5142–5148. [PubMed: 15896062]
32. Fukushima S, Miyata K, Nishiyama N, Kanayama N, Yamasaki Y, Kataoka K. PEGylated polyplex micelles from triblock cationomers with spatially ordered layering of condensed pDNA and buffering units for enhanced intracellular gene delivery. *J. Amer. Chem. Soc.* 2005; 127(9):2810–2811. [PubMed: 15740090]
33. Oishi M, Kataoka K, Nagasaki Y. pH-responsive three-layered PEGylated polyplex micelle based on a lactosylated ABC triblock copolymer as a targetable and endosome-disruptive nonviral gene vector. *Bioconjugate Chem.* 2006; 17(3):677–688.
34. Kanayama N, Fukushima S, Nishiyama N, Itaka K, Jang WD, Miyata K, Yamasaki Y, Chung UI, Kataoka K. A PEG-based biocompatible block cationomer with high buffering capacity for the construction of polyplex micelles showing efficient gene transfer toward primary cells. *Chemmedchem.* 2006; 1(4):439–444. [PubMed: 16892379]
35. Park MR, Han KO, Han IK, Cho MH, Nah JW, Choi YJ, Cho CS. Degradable polyethylenimine-alt-poly(ethylene glycol) copolymers as novel gene carriers. *J. Control. Release.* 2005; 105(3):367–380. [PubMed: 15936108]
36. Bikram M, Ahn CH, Chae SY, Lee MY, Yockman JW, Kim SW. Biodegradable poly(ethylene glycol)-co-poly(L-lysine)-g-histidine multiblock copolymers for nonviral gene delivery. *Macromolecules.* 2004; 37(5):1903–1916.
37. Ahn CH, Chae SY, Bae YH, Kim SW. Biodegradable poly (ethylenimine) for plasmid DNA delivery. *J. Control. Release.* 2002; 80(1–3):273–282. [PubMed: 11943404]
38. Gary DJ, Sharma R, Lee J-S, Jia D, Wan L, Mao G, Konieczny SF, Won Y-Y. In Vitro Gene Silencing and Characterization of ABC Triblock Copolymer Micelleplexes for siRNA Delivery. *J. Control. Release.* 2008 submitted.
39. Baker TS, Olson NH, Fuller SD. Adding the third dimension to virus life cycles: Three-dimensional reconstruction of icosahedral viruses from cryo-electron micrographs. *Microbiol. Mol. Biol. Rev.* 1999; 63(4):862. [PubMed: 10585969]
40. We believe the observed dependence of the DNA intensity at the loading position on the N:P ratio reflects the following three phenomena. (i) At low N:P ratios, where only a fraction of DNA molecules are complexed with polycation segments, the intensity of the band at the loading point signifies the degree of DNA complexation, and therefore, the band shows an increase in intensity with increasing N:P ratio. (ii) On the high-N:P side (i.e., once all DNA molecules are fully complexed), the intensity decreases with the N:P ratio, because at a higher N:P ratio, DNA binds stronger to polycations, which makes it more difficult for the DNA-staining agent (ethidium bromide or EtBr) to intercalate with DNA. (iii) It is documented in the literature that the presence of agglomeration among DNA-polycation complexes can further suppress the EtBr intercalation; see, for instance, Funhoff et al. (*Pharm. Res.* **2004**, 21, 170), Bieber et al. (*J. Control. Release* **2002**, 82, 441), or Ref. 55 cited below. This effect is also observed in our experiments; in the PDMAEMA polyplex and micelleplex cases (i.e., in Figures 2(C) and 2(A), respectively), the DNA signal at the loading position becomes significantly reduced at N:P = 2, where the polyplexes/micelleplexes form larger agglomerates (as shown in the DLS data of Figure 3).
41. Gaehtgens P. Flow of Blood through Narrow Capillaries - Rheological Mechanisms Determining Capillary Hematocrit and Apparent Viscosity. *Biorheology.* 1980; 17(1–2):183–189. [PubMed: 7407348]
42. Rejman J, Oberle V, Zuhorn IS, Hoekstra D. Size-dependent internalization of particles via the pathways of clathrin-and caveolae-mediated endocytosis. *Biochem. J.* 2004; 377:159–169. [PubMed: 14505488]
43. Hansma HG, Golan R, Hsieh W, Lollo CP, Mullen-Ley P, Kwok D. DNA condensation for gene therapy as monitored by atomic force microscopy. *Nucleic Acids Res.* 1998; 26(10):2481–2487. [PubMed: 9580703]

44. Martin AL, Davies MC, Rackstraw BJ, Roberts CJ, Stolnik S, Tendler SJB, Williams PM. Observation of DNA-polymer condensate formation in real time at a molecular level. *FEBS Lett.* 2000; 480:106–112. [PubMed: 11034309]
45. Schellman JA, Parthasarathy N. X-Ray-Diffraction Studies on Cation-Collapsed DNA. *J. Mol. Biol.* 1984; 175(3):313–329. [PubMed: 6726812]
46. Bloomfield VA, Wilson RW, Rau DC. Polyelectrolyte effects in DNA condensation by polymers. *Biophys. Chem.* 1980; 11:339–343. [PubMed: 7407329]
47. Zelphati O, Uyechi LS, Barron LG, Szoka FC. Effect of serum components on the physico-chemical properties of cationic lipid/oligonucleotide complexes and on their interactions with cells. *Biochim. Et Biophys. Acta-Lipids Lipid Metabol.* 1998; 1390(2):119–133.
48. Capan Y, Woo BH, Gebrekidan S, Ahmed S, DeLuca PP. Stability of poly(L-lysine)-complexed plasmid DNA during mechanical stress and DNase I treatment. *Pharm. Dev. Technol.* 1999; 4(4): 491–498. [PubMed: 10578502]
49. Ladiwala A, Rege K, Breneman CM, Kramer SM. A priori prediction of adsorption isotherm parameters and chromatographic behavior in ion-exchange systems. *Proc. Natl. Acad. Sci. U. S. A.* 2005; 102(33):11710–11715. [PubMed: 16081542]
50. Tsuchida E, Osada Y. Role of Chain-Length in Stability of Polyion Complexes. *Makromolekulare Chemie-Macromol. Chem. Phys.* 1974; 175(2):593–601.
51. Tamkovich SN, Cherepanova AV, Kolesnikova EV, Rykova EY, Pyshnyi DV, Vlassov VV, Laktonov PP. Circulating DNA and DNase activity in human blood. *Circulating Nucleic Acids in Plasma and Serum IV.* 2006; Vol. 1075:191–196.
52. Oupicky D, Parker AL, Seymour LW. Laterally stabilized complexes of DNA with linear reducible polycations: Strategy for triggered intracellular activation of DNA delivery vectors. *J. Amer. Chem. Soc.* 2002; 124(1):8–9. [PubMed: 11772047]
53. Lee ES, Na K, Bae YH. Super pH-sensitive multifunctional polymeric micelle. *Nano Lett.* 2005; 5(2):325–329. [PubMed: 15794620]
54. Lynn DM, Langer R. Degradable poly(beta-amino esters): Synthesis, characterization, and self-assembly with plasmid DNA. *J. Amer. Chem. Soc.* 2000; 122(44):10761–10768.
55. Liu XH, Yang JW, Miller AD, Nack EA, Lynn DM. Charge-shifting cationic polymers that promote self-assembly and self-disassembly with DNA. *Macromolecules.* 2005; 38(19):7907–7914.
56. Ooya T, Choi HS, Yamashita A, Yui N, Sugaya Y, Kano A, Maruyama A, Akita H, Ito R, Kogure K, Harashima H. Biocleavable polyrotaxane - Plasmid DNA polyplex for enhanced gene delivery. *J. Amer. Chem. Soc.* 2006; 128(12):3852–3853. [PubMed: 16551060]
57. He YY, Lodge TP. The micellar shuttle: Thermoreversible, intact transfer of block copolymer micelles between an ionic liquid and water. *J. Amer. Chem. Soc.* 2006; 128(39):12666–12667. [PubMed: 17002358]

**Figure 1.**

Representative cryogenic transmission electron microscopy (cryo-TEM) image obtained from an aqueous solution containing the PEG-PnBA-PDMAEMA terpolymer micelles at a concentration of 0.27 mg/ml in 10 mM Tris-HCl buffer (pH 7.5). The cores of the micelles, which appear as dark circles in the image, have a fairly uniform diameter of 19 ± 5 nm. Scale bar represents 110 nm.

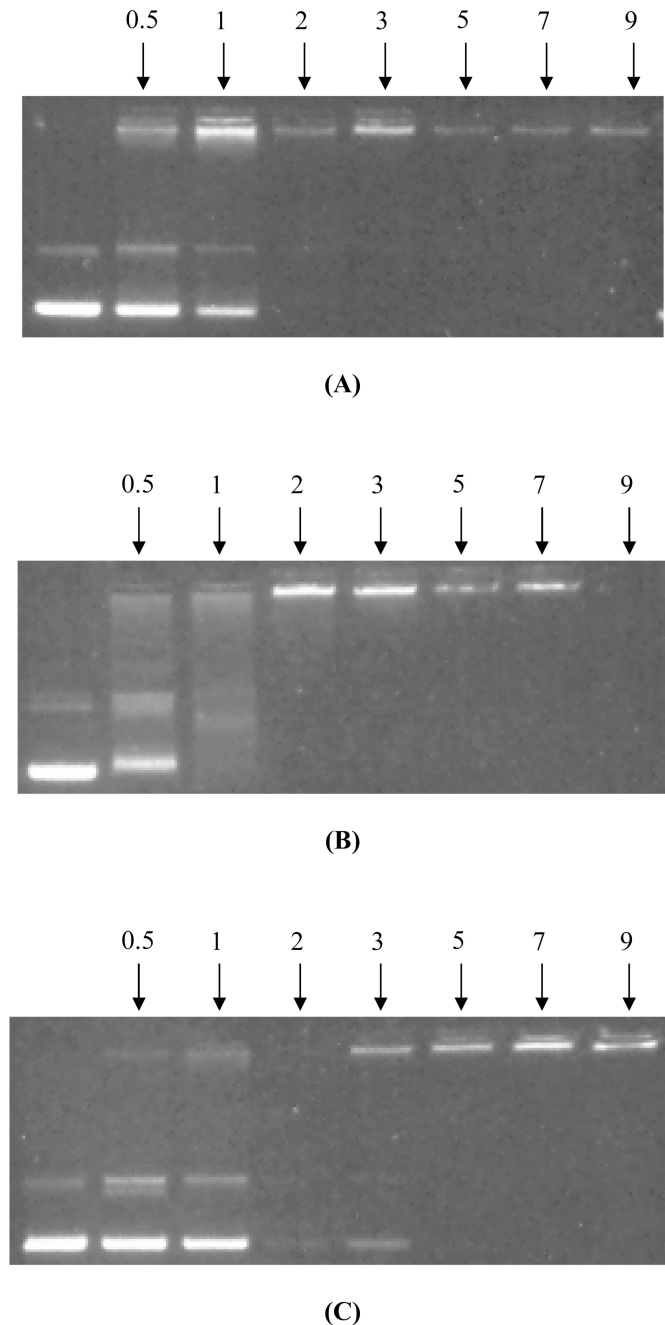
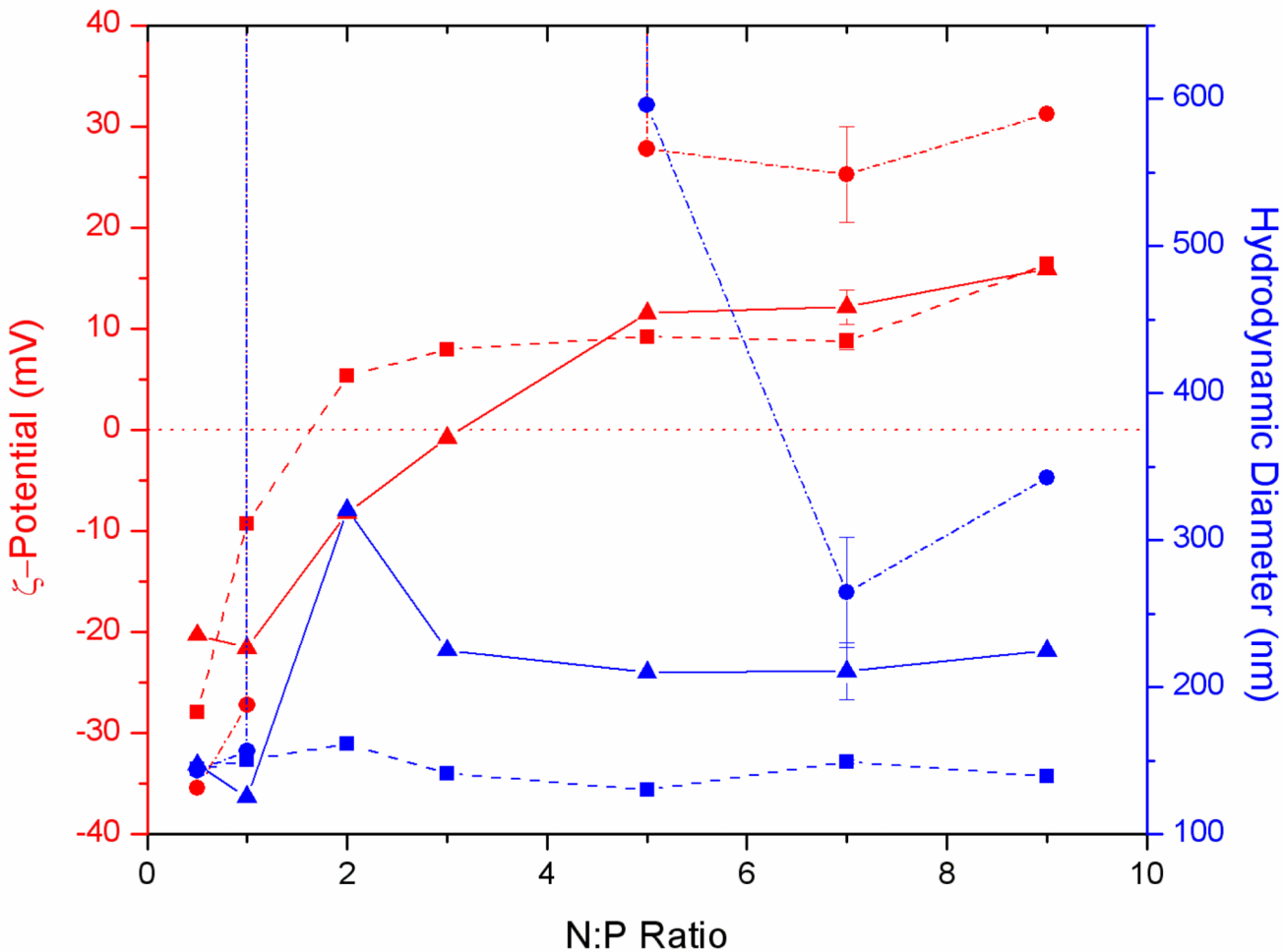


Figure 2.

Electrophoretic mobilities of the pGL-1 plasmid DNA molecules, complexed with (A) the terpolymer micelles, (B) the PEG-PDMAEMA diblock copolymer molecules, and (C) the PDMAEMA homopolymer molecules, at a fixed pGL-1 concentration of 50 µg/ml and seven different N:P ratios as indicated on the top of the lanes. In each panel, the leftmost lane represents the migration of the uncomplexed pGL-1 marker.

**Figure 3.**

Plots of the mean ζ -potentials (red) and hydrodynamic diameters (blue) of the DNA (pGL-1) micelleplexes (\blacktriangle), PEG-PDMAEMA polyplexes (\blacksquare) and PDMAEMA polyplexes (\bullet) as functions of the N:P ratio. All samples were prepared in 10 mM Tris-HCl buffer (pH 7.5) at a fixed pGL-1 concentration of 50 μ g/ml. Representative error bars (which represent standard deviations of triplicate measurements) are shown for the data at N:P = 7. The dotted horizontal line denotes the point of net zero charge (i.e., $\zeta = 0$). No data could be obtained for the PDMAEMA homopolymer-based polyplexes at N:P = 1 and 2, because of the rapid aggregation and precipitation of the polyplexes that occurred during the course of sample preparation.

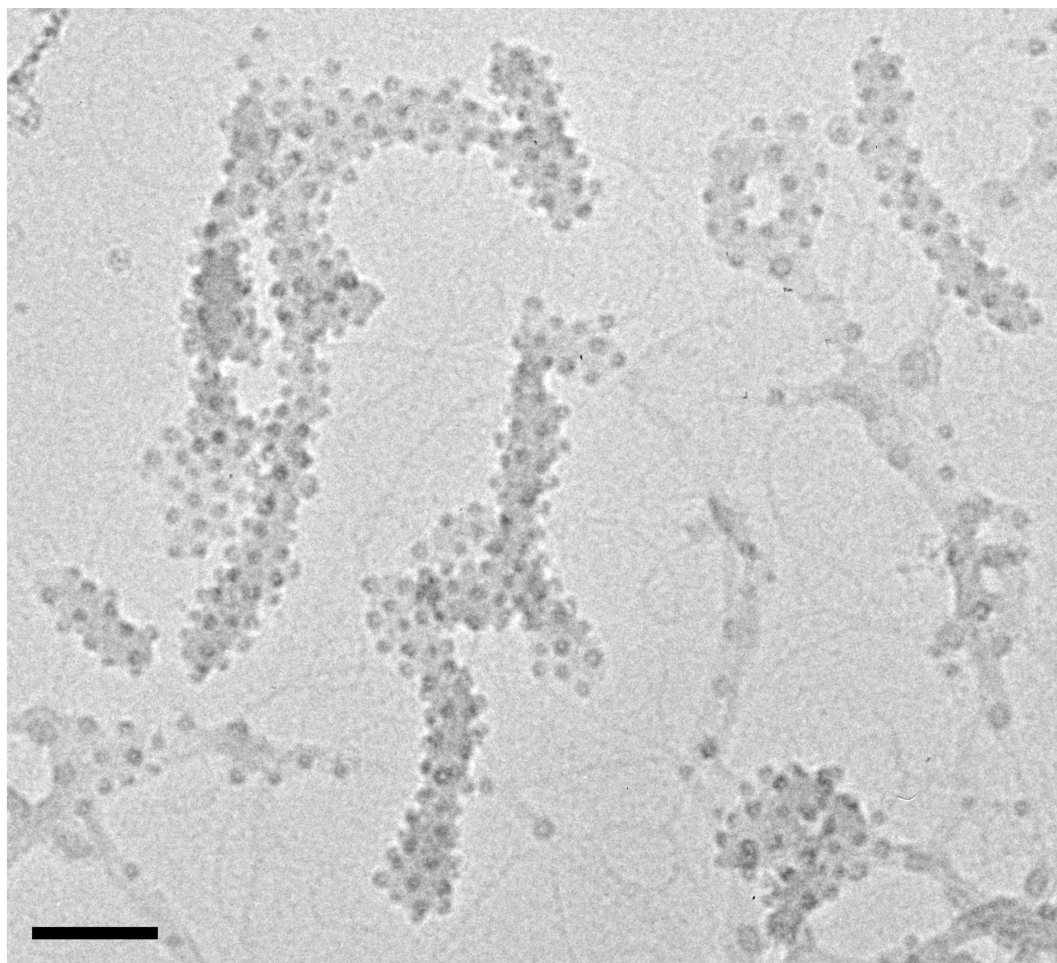
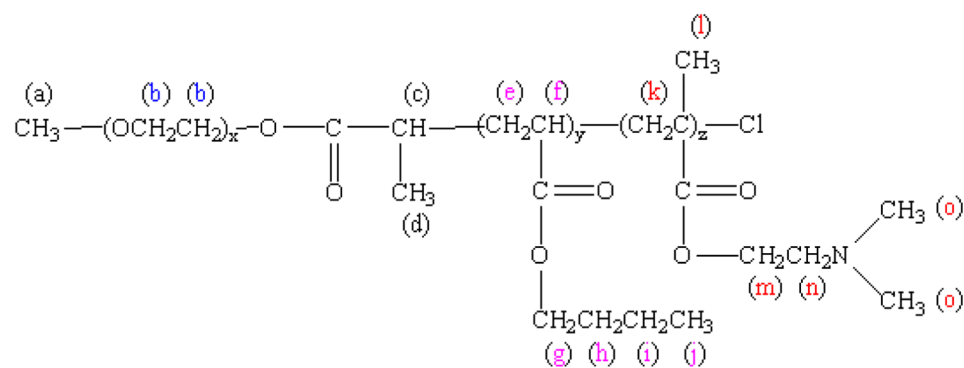
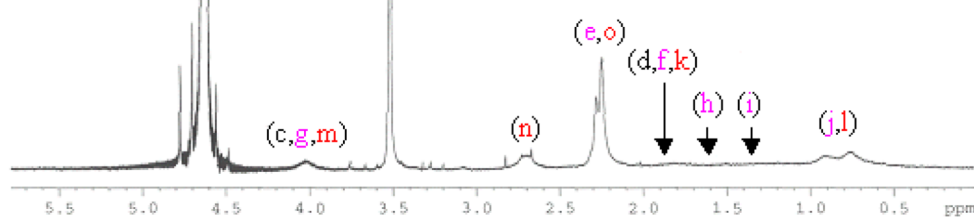
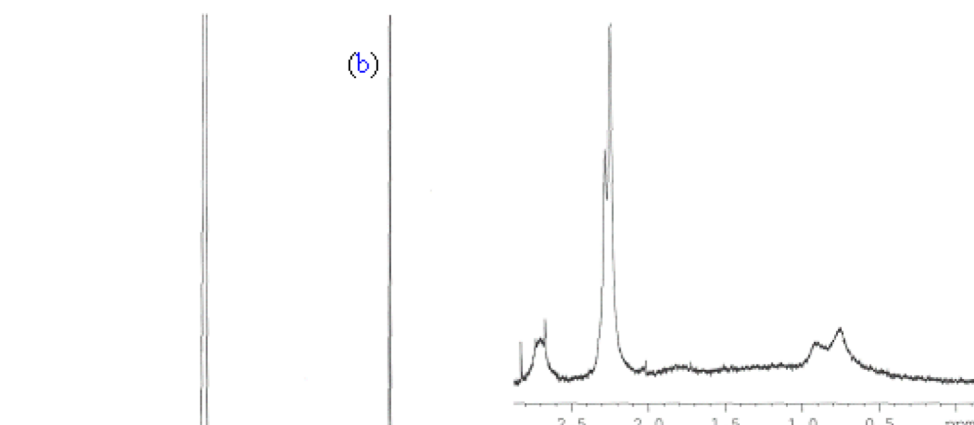


Figure 4.

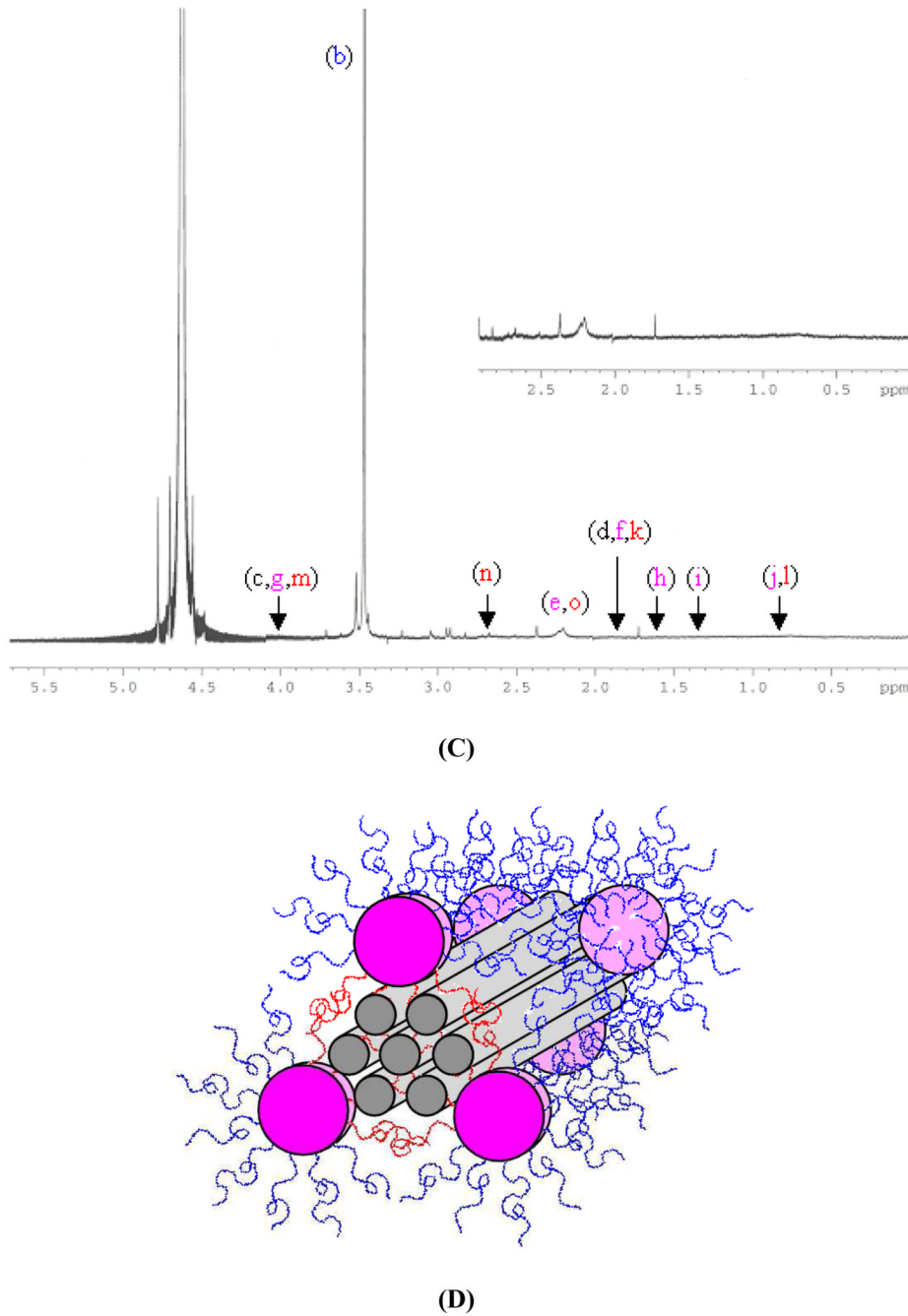
Representative cryogenic transmission electron microscopy (cryo-TEM) image taken from a micelleplex solution, containing 50 µg/ml plasmid DNA (pGL-1) in 10 mM Tris-HCl buffer (pH 7.5), prepared at an N:P ratio of 7:1. Upon complexation with the triblock copolymer micelles (which appear as dark spheres with an apparent diameter of ~ 19 nm in the image), the DNA molecules condense into compact structures. Various condensed DNA morphologies are observed, including multi-stranded bundles, toroids and globules, to name them in the order of their abundance. Scale bar represents 102 nm.



(A)

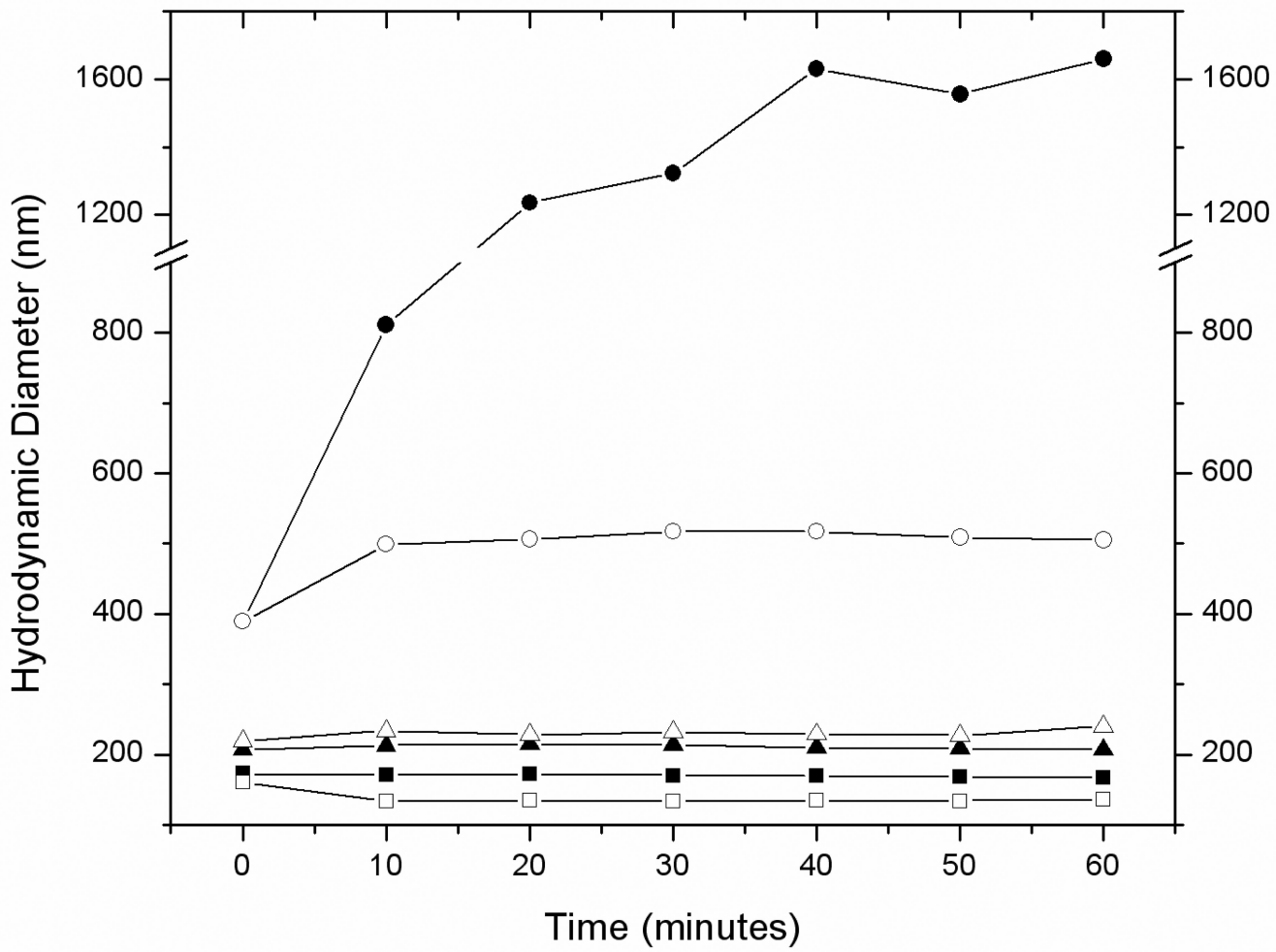


(B)

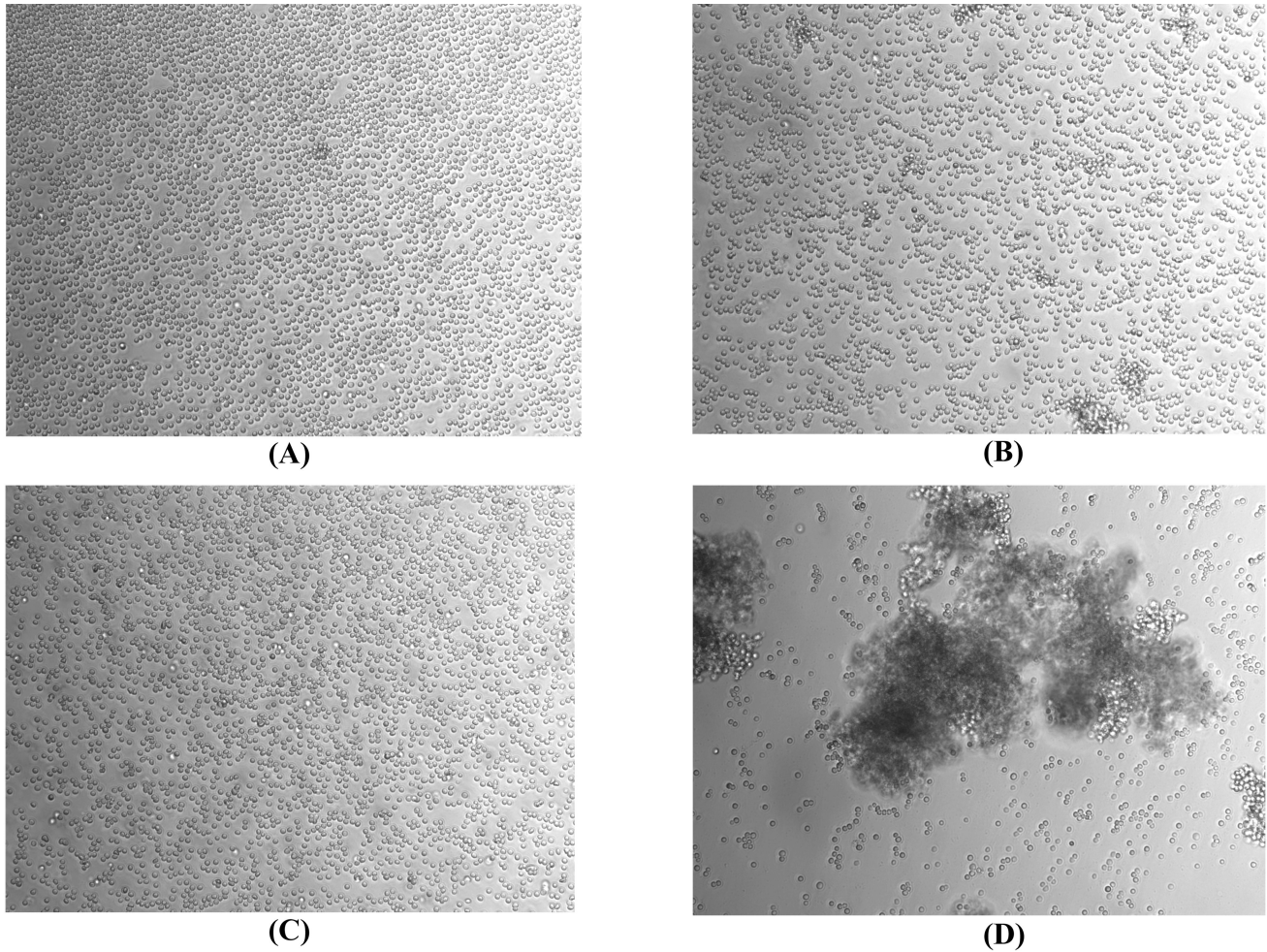
**Figure 5.**

(A) Nomenclature for the protons of the PEG-PnBA-PDMAEMA triblock copolymer.
 (B) ¹H NMR data obtained from a solution containing PEG-PnBA-PDMAEMA micelles at a concentration of 0.91 mg/ml in 10 mM deuterated Tris-HCl buffer. The spectra do not show any signal assignable to the PnBA protons, confirming complete collapse of the PnBA chains into the micelle core domain; see Figure 1(A) for comparison with the NMR spectra for the same triblock polymer molecularly dissolved in CDCl₃. In contrast, the PEG and PDMAEMA chains in the corona give rise to sharp signals at expected chemical shifts. Analysis of the areas of these peaks suggests that about two-thirds of the PDMAEMA

segments are incorporated in the hydrophobic core of the micelle. The strong resonance at around 4.6 ppm is due to trace water (H_2O) in the sample. (C) ^1H NMR spectra for a solution of micelleplexes prepared in the same deuterated buffer, initially at a pGL-1 concentration of 50 $\mu\text{g}/\text{ml}$ and an N:P of 7:1 and then concentrated by a factor of 3.32, which gives final pGL-1 and micelle concentrations of 166 $\mu\text{g}/\text{ml}$ and 0.91 mg/ml, respectively. The (effective) area under the peaks associated with the PDMAEMA chains is decreased by ~ 88% upon complexation with the DNA molecules. (D) Cartoon illustrating the conformations of the PEG and PDMEMA chains in the micelleplex assembly deduced from the NMR data shown in (B) and (C). The blue, pink and red colors respectively denote the PEG, PnBA and PDMAEMA segments of the triblock copolymer. The complexation involves rearrangements of the brush chains, and as a result, the majority of PDMAEMA chains orient towards the interior of the micelleplex, while the PEG chains predominantly occupy the outer surface of the micelleplex structure.

**Figure 6.**

Stability against aggregation of the micelleplexes (\blacktriangle), PEG-PDMAEMA polyplexes (\blacksquare) and PDMAEMA polyplexes (\bullet) in the presence of 150 mM salt (filled symbols) or 40 mg/ml albumin (open symbols). All complexes were prepared at N:P = 7 in 10 mM Tris-HCl buffer at a DNA concentration of 50 μ g/ml. An appropriate amount of 1.5 M PBS or BSA solution (200 mg/ml in 10 mM Tris-HCl buffer) was added to the respective complex solution at $t=0$, and afterwards the sizes of the complexes were measured by DLS.

**Figure 7.**

Bright field optical microscopy images ($348\mu\text{m} \times 261\mu\text{m}$) of bovine erythrocytes (red blood cells) in 150 mM CMF saline after 2 hours of incubation (A) with no added polymer-DNA complexes, (B) with the micelleplexes, (C) with the PEG-PDMAEMA polyplexes, and (D) with the PDMAEMA polyplexes. All complexes were prepared at N:P = 7 in 10 mM Tris-HCl buffer at a DNA concentration of 50 $\mu\text{g/ml}$.

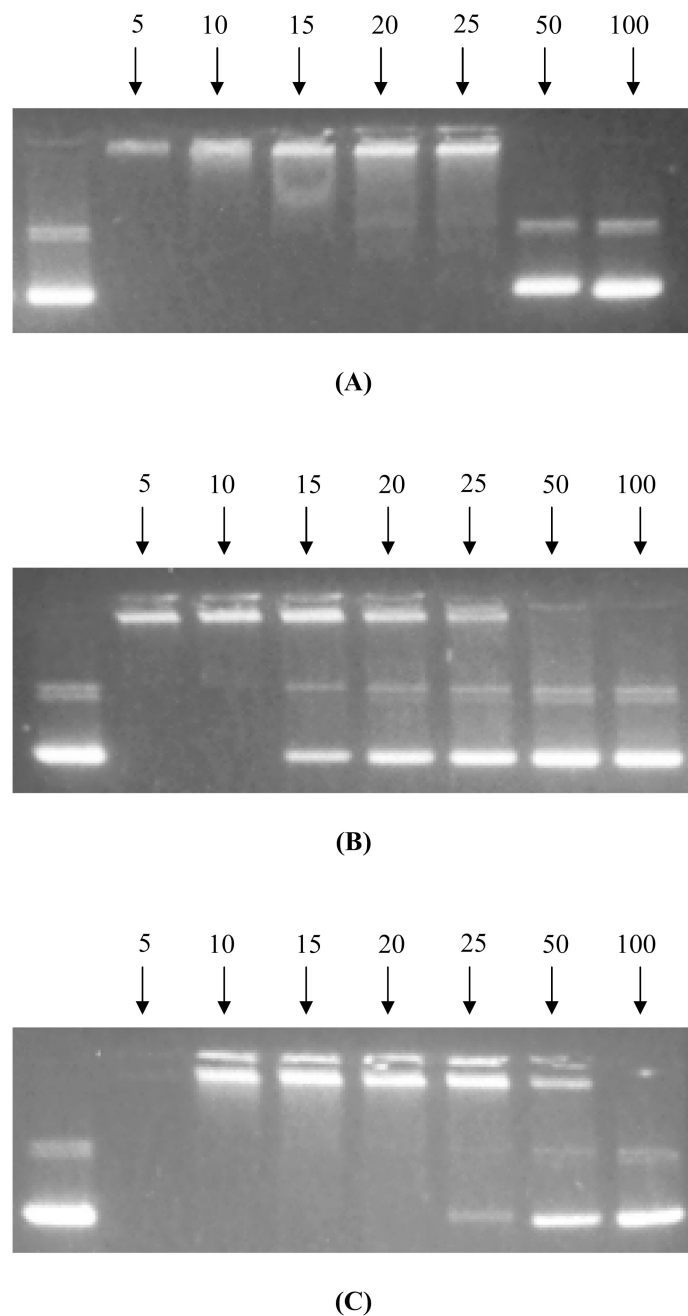
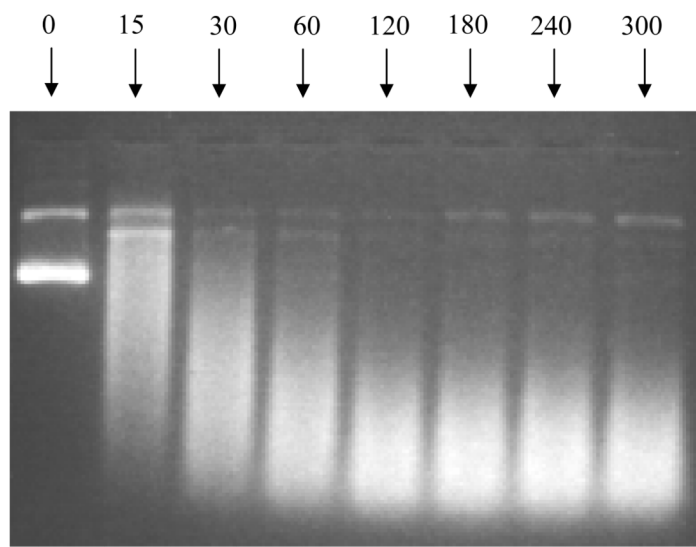
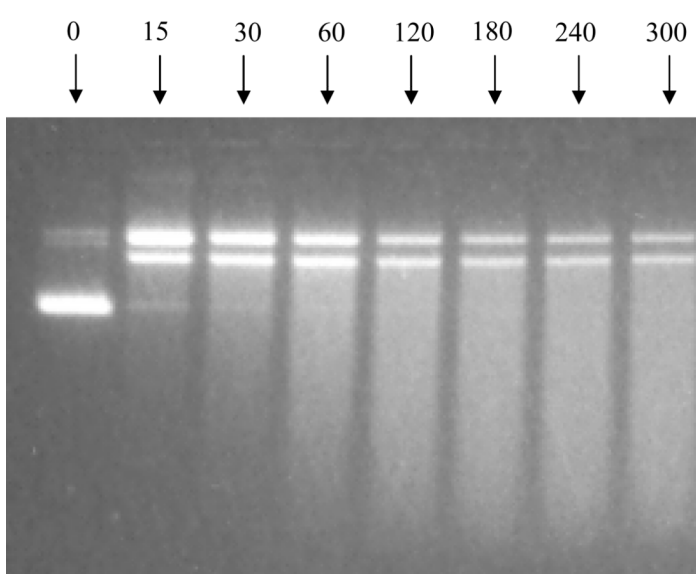


Figure 8.
Agarose gel electrophoresis data demonstrating how the (A) micelleplexes, (B) PEG-PDMAEMA polyplexes and (C) PDMAEMA polyplexes become dissociated by added anionic poly(aspartic acid) (PAA) at various PAA concentrations. Each micelleplex/polyplex sample was prepared to contain 50 μ g/ml pGL-1 DNA at 7:1 N:P ratio, and was exposed to PAA for 24 hours at room temperature under constant agitation before the electrophoresis analysis. As one goes from the second most-left lane to the rightmost lane, the PAA concentration increases from an A:P ratio (defined as $[COO^-]/[PO_4^{3-}]$) of 5 to 10, 15, 20, 25, 50 and 100 (as indicated on top of the lanes). Shown in the left-most column are

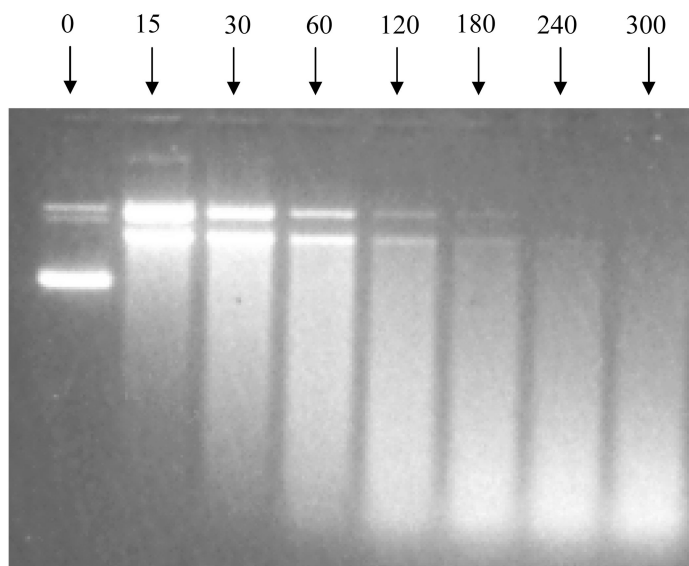
the separation bands of pristine pGL-1 which is used as a marker for complete dissociation of the DNA from the respective complex.



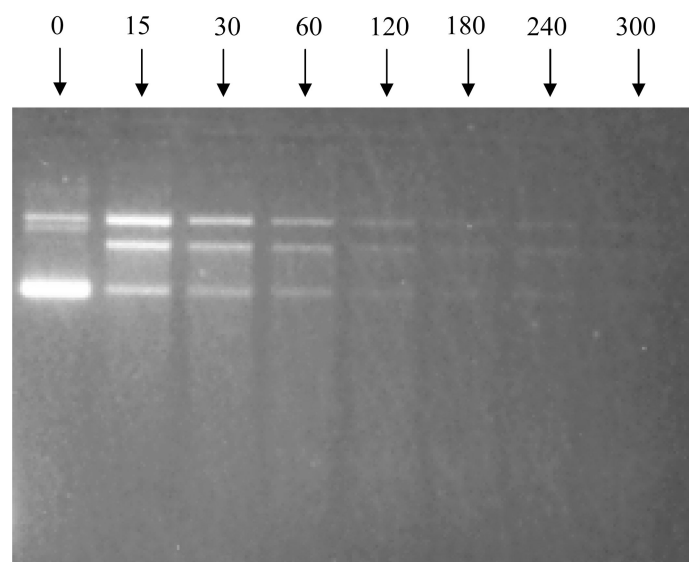
(A)



(B)



(C)



(D)

Figure 9.

Agarose gel electrophoresis data demonstrating how (A) the unprotected pGL-1, and the same DNA complexed with (B) the triblock copolymer micelle, (C) PEG-PDMAEMA diblock copolymer and (D) PDMAEMA homopolymer (all at N:P = 7) become degraded by exposure to DNase I as functions of the exposure time. All samples were prepared at a pGL-1 concentration of 50 µg/ml in 10 mM Tris-HCl buffer (pH 7.5). The samples were exposed to DNase I for various exposure times (as indicated (in minutes) above the lanes), and in the micelleplex/polyplex cases the DNA samples were further treated with PAA (A:P

= 100) at room temperature for 24 hours (for separation of the DNA from the complex), prior to the gel electrophoresis.

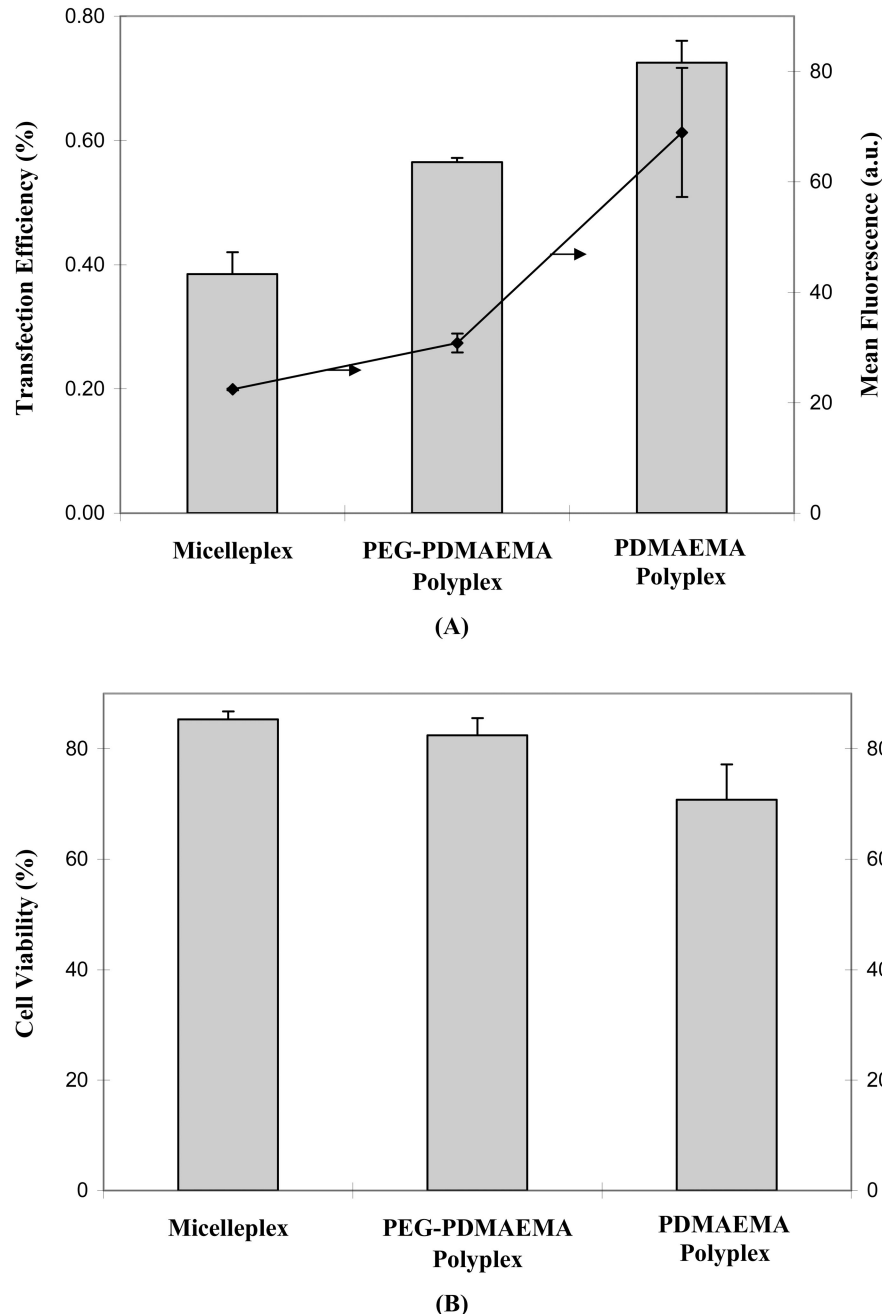
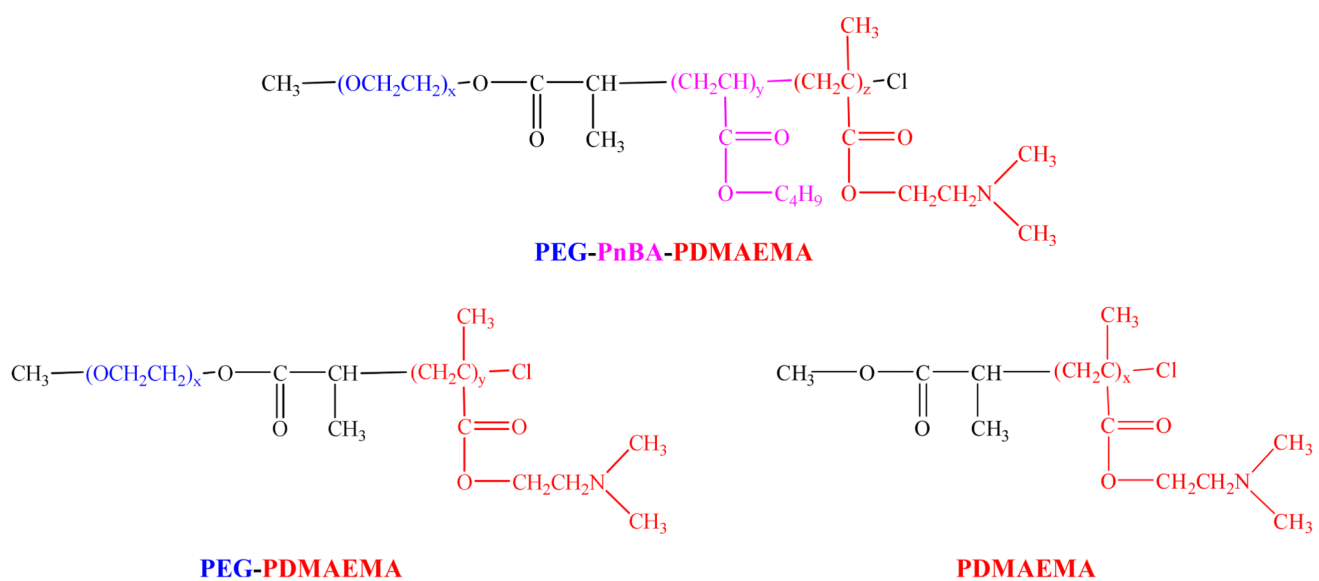


Figure 10.

(A) Gene transfection efficiencies of the micelleplexes, PEG-PDMAEMA polyplexes and PDMAEMA polyplexes in HeLa cells. All complexes were prepared at N:P = 7 using GFP-encoding pGL-1 as the reporter gene (at a pGL-1 concentration of 50 µg/ml). The transfection efficiency of each complex was determined by flow cytometry as the fraction of total gated cells that show higher GFP fluorescence intensities than the autofluorescence level of the pristine HeLa cells. Also shown with filled circles are the average fluorescence intensities per cell from the GFP-expressing cells for the different DNA complexes. Error bars represent the standard deviations of the means. (B) Normalized viability of the HeLa

cells transfected respectively with the micelleplexes, PEG-PDMAEMA polyplexes and PDMAEMA polyplexes determined by MTT assay. All conditions were the same as in the gene transfection assay. All measurements were done in triplicates. Error bars represent the standard deviations.

**Scheme 1.**

Chemical structures of the polymers used in this study.

Table 1

Molecular weight and polydispersity characteristics of the polymers used in this study.

Polymer	DP _{n,PEG} [*]	DP _{n,PnBA} [*]	DP _{n,PDMAEMA} [*]	PDI [#]
PEG-PnBA-PDMAEMA	113	100	128	1.29
PEG-PDMAEMA	113	-	142	1.23
PDMAEMA	-	-	127	1.18

^{*} DP_{n,PEG}, DP_{n,PnBA} and DP_{n,PDMAEMA} denote the number-average degrees of polymerization of the PEG, PnBA and PDMAEMA component blocks, respectively, as determined by ¹H NMR spectroscopy.

[#] Polydispersity indices determined by gel permeation chromatography (GPC) using polystyrene molecular weight standards.